is positively regulated by c/EBPα but not c/EBPβ (Hansen et al., 1998; Plumb-Rudewiez et al., 2004), suggesting that the functions of c/EBPα and c/EBPβ in the hepatoblast fate decision might be different.

In the present study, we first examined the function of TGFBR2 in the hepatoblast fate decision using hESC-derived hepatoblast-like cells, which have the ability to self-replicate, differentiate into both hepatocyte and cholangiocyte lineages, and repopulate the liver of carbon tetrachloride (CCl_4)-treated immunodeficient mice. *In vitro* gain- and loss-of-function analyses and *in vivo* transplantation analysis were performed. Next, we investigated how TGFBR2 expression is regulated in the hepatoblast fate decision. Finally, we examined whether our findings could be reproduced in delta-like 1 homolog (Dlk1)-positive hepatoblasts obtained from the liver of E13.5 mice. To the best of our knowledge, this study provides the first evidence of c/EBP-mediated regulation of TGFBR2 expression in the human hepatoblast fate decision.

RESULTS

Hepatoblast-like cells are generated from hESCs

First, we investigated whether the hepatoblast-like cells (HBCs), which were differentiated from hESCs as described in supplementary material Fig. S1A, have similar characteristics to human hepatoblasts. We recently found that hESC-derived HBCs could be purified and maintained on human laminin 111 (LN111)-coated dishes (Takayama et al., 2013). The long-term cultured HBC population (HBCs passaged more than three times were used in this study) were nearly homogeneous and expressed human hepatoblast markers such as alpha-fetoprotein (AFP), albumin (ALB), cytokeratin 19 (CK19, also known as KRT19) and EPCAM (Schmelzer et al., 2007) (supplementary material Fig. S1B). In addition, most of the colonies observed on human LN111-coated plates were ALB and CK19 double positive, although a few colonies were ALB single positive, CK19 single positive, or ALB and CK19 double negative (supplementary material Fig. S1C). To examine the hepatocyte differentiation capacity of the HBCs *in vivo*, these cells were transplanted into CCl_4-treated immunodeficient mice. The hepatocyte functionality of the transplanted cells was assessed by measuring secreted human ALB levels in the recipient mice (supplementary material Fig. S1D). Human ALB serum was detected in the mice that were transplanted with the HBCs, but not in the control mice. These results demonstrated that the HBCs generated from hESCs have similar characteristics to human hepatoblasts and would therefore provide a valuable tool to investigate the mechanisms of human liver development. In the present study, HBCs generated from hESCs were used to elucidate the mechanisms of the hepatoblast fate decision.

TGFBR2 expression is decreased in hepatocyte differentiation but increased in cholangiocyte differentiation

The HBCs used in this study have the ability to differentiate into both hepatocyte-like cells [cytochrome P450 3A4 (CYP3A4) positive; Fig. 1B] and cholangiocyte-like cells (CK19 positive; Fig. 1C) (the protocols are described in Fig. 1A). Because the expression pattern of TGFBR2 during differentiation from hepatoblasts is not well known, we examined it in hepatocyte and cholangiocyte differentiation from HBCs. *TGFBR2* was downregulated during hepatocyte differentiation from HBCs (Fig. 1D), but upregulated in cholangiocyte differentiation from HBCs (Fig. 1E). After the HBCs were cultured on Matrigel, the cells were fractionated into three populations according to the level of TGFBR2 expression (TGFBR2-negative, -lo or -hi; Fig. 1F). The HBC-derived TGFBR2-lo cells strongly expressed *αAT* and *CYP3A4* (hepatocyte markers), whereas the HBC-derived TGFBR2-hi cells strongly expressed *SOX9* and integrin β4 (*ITGB4*) (cholangiocyte markers). These data suggest that the TGFBR2 expression level is decreased in hepatic differentiation, but increased in biliary differentiation of the HBCs.

The cell fate decision of HBCs is regulated by TGFβ signals

To examine the function of TGFβ1, β2 and β3 (all of which are ligands of TGFBR2) in the hepatoblast fate decision, HBCs were cultured in medium containing TGFβ1, β2 or β3 (Fig. 2A,B). The expression levels of cholangiocyte marker genes were upregulated by addition of TGFβ1 or TGFβ2, but not TGFβ3 (Fig. 2A), whereas those of hepatocyte markers were downregulated by addition of TGFβ1 or TGFβ2 (Fig. 2B). To ascertain that TGFBR2 is also important in the hepatoblast fate decision, HBCs were cultured in medium containing SB-431542, which inhibits TGFβ signaling (Fig. 2C,D). Hepatocyte marker genes were upregulated by inhibition of TGFβ signaling (Fig. 2C), whereas cholangiocyte markers were downregulated (Fig. 2D). To confirm the function of TGFβ1, β2 and β3 in the hepatoblast fate decision, colony assays of the HBCs were performed in the presence or absence of TGFβ1, β2 or β3 (Fig. 2E). The number of CK19 single-positive colonies was significantly increased in TGFβ1- or β2-treated HBCs. By contrast, the number of ALB and CK19 double-positive colonies was reduced in TGFβ1-, β2- or β3-treated HBCs. These data indicated that TGFβ1 and β2 positively regulate the biliary differentiation of HBCs. Taken together, the findings suggested that TGFBR2 might be a key molecule in the regulation of hepato-bilary lineage segregation.

TGFBR2 plays an important role in the cell fate decision of HBCs

To examine whether TGFBR2 plays an important role in the hepatoblast fate decision, *in vitro* gain- and loss-of-function analysis of TGFBR2 was performed in the HBCs. We used siRNA in knockdown experiments (supplementary material Fig. S2) during HBC differentiation on Matrigel. Whereas TGFBR2-suppressing siRNA (si-TGFBR2) transfection upregulated the expression of hepatocyte markers, it downregulated cholangiocyte markers (Fig. 3A). si-TGFBR2 transfection increased the percentage of asialoglycoprotein receptor 1 (ASGR1)-positive hepatocyte-like cells (Fig. 3B). By contrast, it decreased the percentage of aquaporin 1 (AQP1)-positive cholangiocyte-like cells. These results suggest that TGFBR2 knockdown promotes hepatocyte differentiation, whereas it inhibits cholangiocyte differentiation. Next, we used Ad vector to perform efficient transduction into the HBCs (supplementary material Fig. S3) and ascertained *TGFBR2* gene expression in TGFBR2-expressing Ad vector (Ad-TGFBR2)-transduced cells (supplementary material Fig. S4). Ad-TGFBR2 transduction downregulated the expression of hepatocyte markers, whereas it upregulated cholangiocyte markers (Fig. 3C). Ad-TGFBR2 transduction decreased the percentage of ASGR1-positive hepatocyte-like cells but increased the percentage of AQP1-positive cholangiocyte-like cells (Fig. 3D). These results suggest that TGFBR2 overexpression inhibits hepatocyte differentiation, whereas it promotes cholangiocyte differentiation. Taken together, these results suggest that TGFBR2 plays an important role in deciding the differentiation lineage of HBCs.

To investigate whether hepatoblasts would undergo differentiation in a TGFBR2-associated manner *in vivo*, HBCs transfected/transduced with si-control, si-TGFBR2, Ad-LacZ or Ad-

Development (2014) doi:10.1242/dev.103168

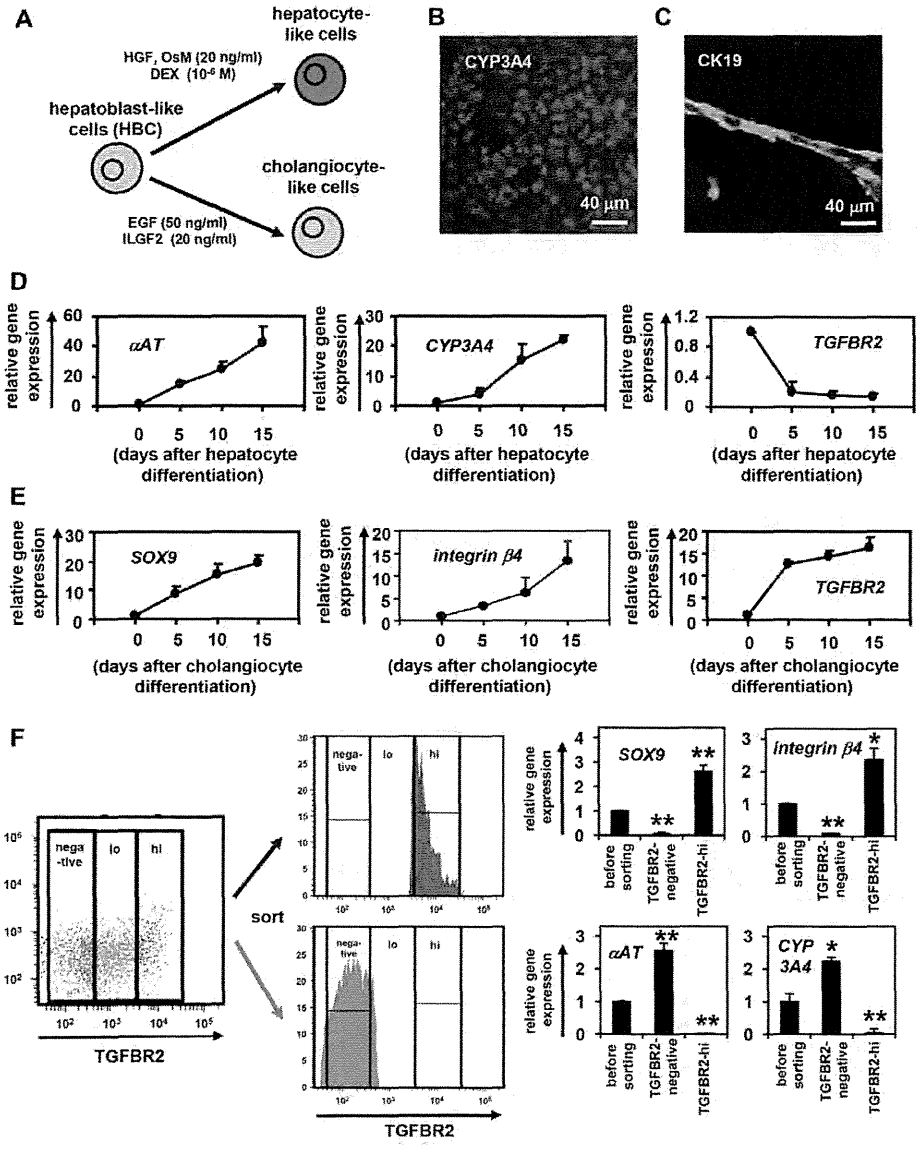

Fig. 1. HBCs can differentiate into both hepatocyte and cholangiocyte lineages. (A) The strategy for hepatocyte and cholangiocyte differentiation from HBCs. (B,C) The HBC-derived hepatocyte-like cells or cholangiocyte-like cells were subjected to immunostaining with anti-CYP3A4 (red, B) or anti-CK19 (green, C) antibodies, respectively. (D,E) Temporal gene expression levels of hepatocyte markers (*αAT* and *CYP3A4*) (D) or cholangiocyte markers (*SOX9* and integrin β4) (E) during hepatocyte or cholangiocyte differentiation as measured by real-time RT-PCR. The temporal gene expression of *TGFBR2* was also examined. The gene expression levels in HBCs were taken as 1.0. (F) HBCs were cultured on Matrigel for 5 days, and then the expression level of TGFBR2 was examined by FACS analysis. TGFBR2-negative, -lo and -hi populations were collected and real-time RT-PCR analysis was performed to measure the expression levels of hepatocyte markers (*αAT* and *CYP3A4*) and cholangiocyte markers (*SOX9* and integrin β4). **P*<0.05, ***P*<0.01 (compared with 'before sorting'). Error bars indicate s.d. Statistical analysis was performed using the unpaired two-tailed Student's *t*-test (n=3).

TGFBR2 were transplanted into CCl_4-treated immunodeficient mice (Fig. 3E,F). Although some of the si-control-transfected or Ad-LacZ-transduced HBCs remained as HBCs (HNF4α and CK19 double positive), most of them showed *in vitro* differentiation toward hepatocyte-like cells (HNF4α single positive) (Fig. 3E, top row). By contrast, Ad-TGFBR2-transduced HBCs were predominantly committed to cholangiocyte-like cells (CK19 single positive) and si-TGFBR2-transfected HBCs were predominantly committed to hepatocyte-like cells (HNF4α single positive) (Fig. 3E, bottom row). Ad-TGFBR2 transduction decreased the percentage of HNF4α-positive hepatocyte-like cells, whereas it increased the percentage of CK19-positive cholangiocyte-like cells (supplementary material Fig. S5). The hepatocyte functionality of the *in vivo* differentiated HBCs was assessed by measuring secreted human ALB levels in the recipient mice (Fig. 3F). Mice that were transplanted with Ad-TGFBR2-transduced HBCs showed lower human ALB serum levels than those transplanted with Ad-LacZ-transduced HBCs, and the mice that were transplanted with si-TGFBR2-transfected HBCs showed higher human ALB serum levels than those transplanted with si-control-transfected HBCs. These data suggest that cholangiocyte or hepatocyte differentiation was promoted by TGFBR2 overexpression or knockdown, respectively. Thus, based on these data from *in vitro* and *in vivo* experiments, TGFBR2 plays an important role in deciding the differentiation lineage of HBCs.

TGFBR2 promoter activity and expression are negatively regulated by c/EBPα and positively regulated by c/EBPβ

A previous study has shown that TGFBR2 expression is upregulated in *Hnf6* knockout mice (Clotman et al., 2005), although we confirmed by ChIP assay that HNF6 does not bind to the *TGFBR2* promoter region (data not shown). Because c/EBPα is important in the hepatoblast fate decision (Suzuki et al., 2003), we expected that c/EBPs might directly regulate TGFBR2 expression. The *TGFBR2* promoter region was analyzed to examine whether TGFBR2 expression is regulated by c/EBPs. Some c/EBP binding sites (supplementary material Fig. S6) were predicted by rVista 2.0 (http://rvista.dcode.org/) (Fig. 4A). By performing a ChIP assay, one

Development (2014) doi:10.1242/dev.103168

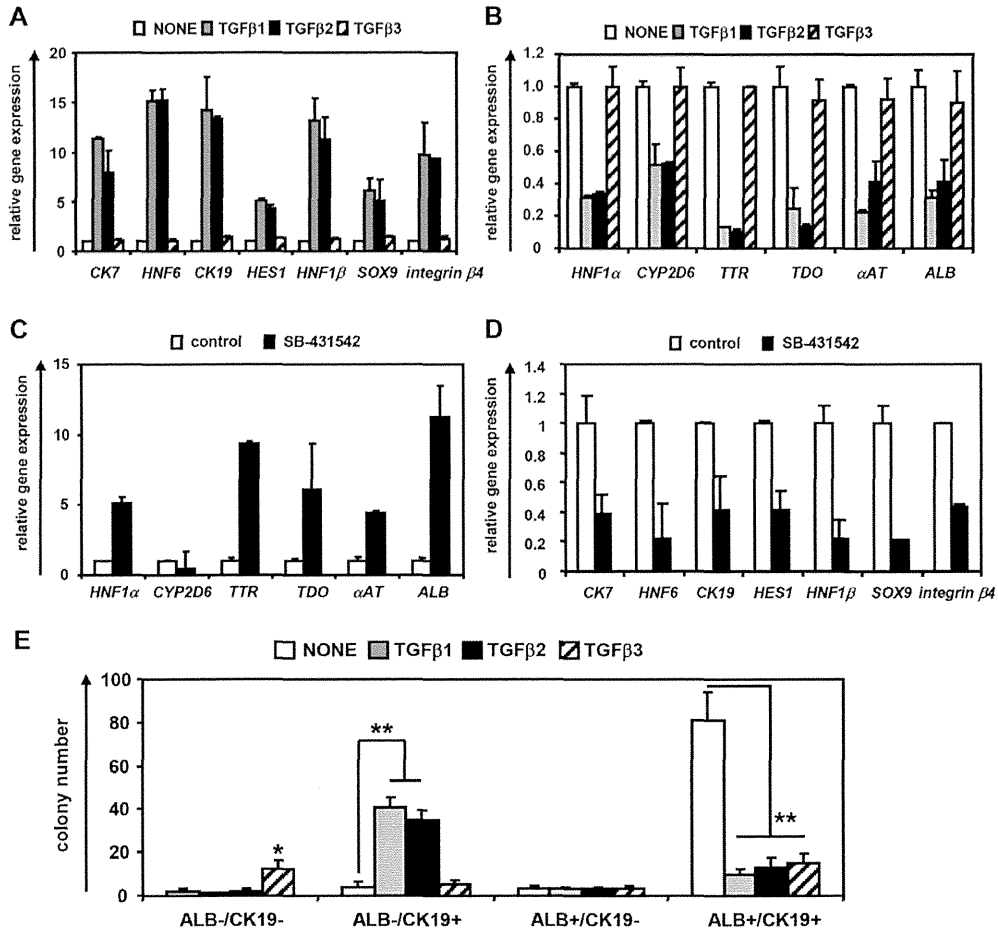

Fig. 2. Hepatocyte and cholangiocyte differentiation from HBCs is regulated by TGFβ signaling. (A,B) HBCs were cultured in differentiation hESF-DIF medium containing 10 ng/ml TGFβ1, TGFβ2 or TGFβ3 for 10 days. The expression levels of cholangiocyte (A) and hepatocyte (B) marker genes were measured by real-time RT-PCR. On the *y*-axis, the gene expression level of cholangiocyte markers in untreated cells (NONE) was taken as 1.0. (C,D) HBCs were cultured in differentiation hESF-DIF medium containing SB-431542 (10 μM) for 10 days. Control cells were treated with solvent only (0.1% DMSO). Expression levels of hepatocyte (C) and cholangiocyte (D) marker genes were measured by real-time RT-PCR. On the *y*-axis, the gene expression level of hepatocyte markers in untreated cells (control) was taken as 1.0. (E) HBC colony formation assay in the presence or absence of 10 ng/ml TGFβ1, TGFβ2 or TGFβ3. HBCs were plated at 200 cells/cm^2 on human LN111-coated dishes. The colonies were separated into four groups based on the expression of ALB and CK19: double-negative, ALB negative and CK19 positive, ALB positive and CK19 negative, and double positive. The numbers represent wells in which the colony was observed in three 96-well plates (total 288 wells). Five days after plating, the cells were fixed with 4% PFA and used for double immunostaining. $^*P<0.05$, $^{**}P<0.01$ (compared with NONE). Error bars indicate s.d. Statistical analysis was performed using the unpaired two-tailed Student's *t*-test ($n=3$).

c/EBP binding site was found in the *TGFBR2* promoter region (Fig. 4B). A reporter assay of the *TGFBR2* promoter region showed that c/EBPβ activates *TGFBR2* promoter activity, whereas c/EBPα inhibits it (Fig. 4C). In addition, *TGFBR2* expression was downregulated by Ad-c/EBPα transduction, whereas *TGFBR2* was upregulated by Ad-c/EBPβ transduction in HepG2 cells (TGFBR2 positive) (Fig. 4D). We ascertained the expression of *c/EBPα* or *c/EBPβ* (*CEBPA* or *CEBPB* – Human Gene Nomenclature Committee) in the Ad-c/EBPα- or Ad-c/EBPβ-transduced cells, respectively (supplementary material Fig. S4). These results demonstrated that the promoter activity and expression of *TGFBR2* were directly regulated by both c/EBPα and c/EBPβ.

c/EBPs determine the cell fate decision of HBCs via regulation of TGFBR2 expression

To elucidate the relationship between TGFBR2 and c/EBPs (c/EBPα and c/EBPβ) in the hepatoblast fate decision, we first examined the temporal gene expression patterns of *TGFBR2*, *c/EBPα* and *c/EBPβ* in hepatocyte and cholangiocyte differentiation. During hepatocyte differentiation, *TGFBR2* expression was downregulated, whereas *c/EBPα* was upregulated (supplementary material Fig. S7A, top). During cholangiocyte differentiation, *c/EBPα* was downregulated, whereas *TGFBR2* and *c/EBPβ* were upregulated (supplementary material Fig. S7A, bottom). In addition, the ratio of *c/EBPα* to *c/EBPβ* was significantly increased in hepatocyte differentiation, but significantly reduced in cholangiocyte differentiation (supplementary material Fig. S7B). High-level expression of *c/EBPα* was detected in TGFBR2-negative cells, but not in TGFBR2-hi cells (supplementary material Fig. S7C). By contrast, high-level expression of *c/EBPβ* was detected in TGFBR2-hi cells, but not in TGFBR2-negative cells. These results suggest that TGFBR2 is negatively regulated by c/EBPα and positively regulated by c/EBPβ in the differentiation model from HBCs as well as in the HepG2 cell line (Fig. 4).

Development (2014) doi:10.1242/dev.103168

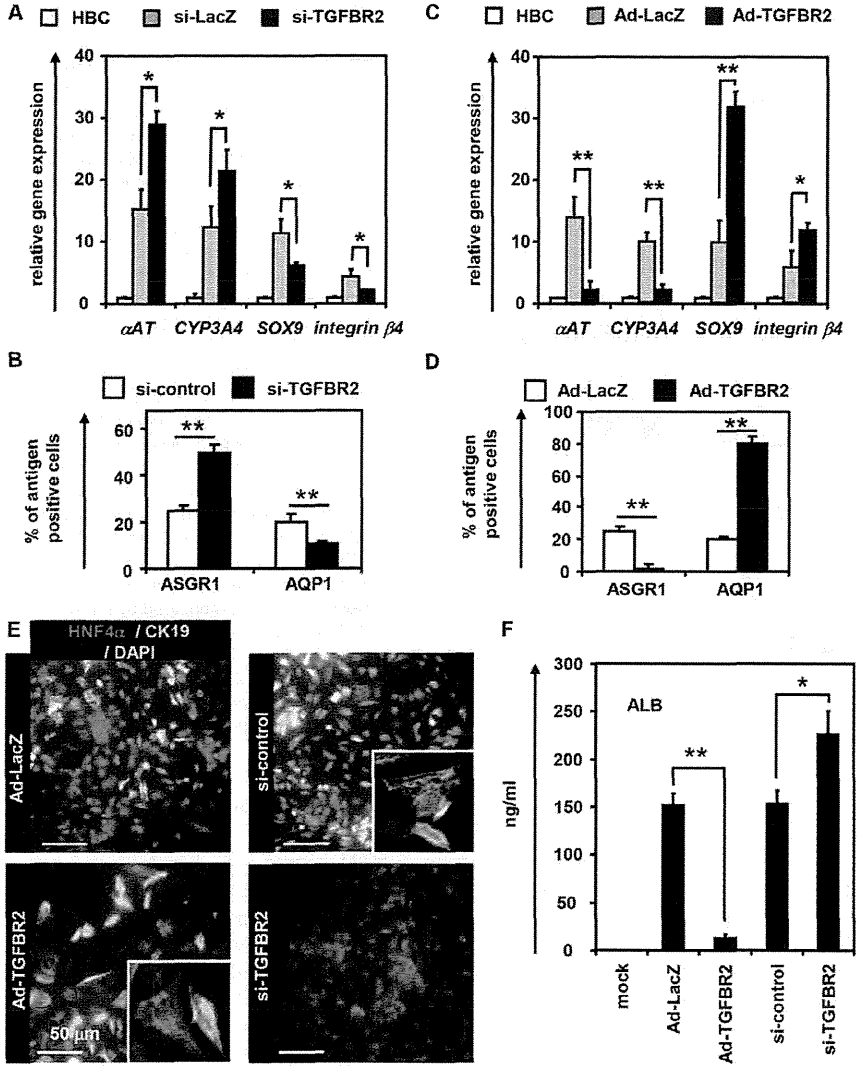

Fig. 3. TGFBR2 regulates bi-directional differentiation of HBCs. (A) HBCs were transfected with 50 nM control siRNA (si-control) or TGFBR2-suppressing siRNA (si-TGFBR2) and cultured in differentiation hESF-DIF medium for 10 days. The expression levels of hepatocyte (*αAT* and *CYP3A4*) or cholangiocyte (*SOX9* and integrin β4) markers were measured by real-time RT-PCR. On the *y*-axis, the gene expression level in HBCs was taken as 1.0. (B) On day 10 after siRNA transfection, the efficiency of hepatocyte or cholangiocyte differentiation was measured by estimating the percentage of ASGR1-positive or AQP1-positive cells, respectively, by FACS analysis. (C) HBCs were transduced with 3000 VPs/cell of Ad-LacZ or Ad-TGFBR2 for 1.5 hours and cultured in differentiation hESF-DIF medium for 10 days. Expression levels of hepatocyte or cholangiocyte marker genes were measured by real-time RT-PCR. On the *y*-axis, gene expression levels in the HBCs was taken as 1.0. (D) On day 10 after Ad vector transduction, the efficiency of hepatocyte or cholangiocyte differentiation was measured by estimating the percentage of ASGR1-positive or AQP1-positive cells, respectively, by FACS analysis. (E,F) The si-control, si-TGFBR2, Ad-LacZ- or Ad-TGFBR2-transfected/transduced HBCs (1.0×10^6 cells) were transplanted into CCl_4-treated (2 mg/kg) *Rag2/Il2rg* double-knockout mice by intrasplenic injection. (E) Expression of human HNF4α (red) and CK19 (green) was examined by double immunohistochemistry 2 weeks after transplantation. Nuclei were counterstained with DAPI (blue). (F) Levels of human ALB in recipient mouse serum were measured 2 weeks after transplantation. **P*<0.05, ***P*<0.01 (compared with Ad-LacZ-transduced or si-control-transfected cells). Error bars indicate s.d. Statistical analysis was performed using the unpaired two-tailed Student's *t*-test (n=3).

ChIP experiments showed that c/EBPα or c/EBPβ is recruited to the *TGFBR2* promoter region containing the c/EBP binding site in hepatocyte-like cells or cholangiocyte-like cells, respectively (Fig. 5A), suggesting that c/EBPα and c/EBPβ oppositely regulate *TGFBR2* promoter activity in the differentiation from HBCs. We confirmed that c/EBPα or c/EBPβ was mainly recruited to the *TGFBR2* promoter region containing the c/EBP binding site in TGFBR-negative or TGFBR2-positive cells, respectively (supplementary material Fig. S7D). Taken together, we concluded that c/EBPα and c/EBPβ are able to regulate the cell fate decision of HBCs via regulation of TGFBR2 expression. During differentiation from HBCs, *TGFBR2* expression was negatively regulated by c/EBPα and positively regulated by c/EBPβ (Fig. 5B). To examine whether c/EBPα or c/EBPβ could regulate the differentiation from HBCs, *in vitro* gain- and loss-of-function analyses were performed. si-c/EBPα transfection downregulated hepatocyte marker gene expression, whereas it upregulated cholangiocyte marker genes (Fig. 5C). By contrast, si-c/EBPβ transfection upregulated hepatocyte marker and downregulated cholangiocyte marker gene expression (Fig. 5C). In accordance, Ad-c/EBPα transduction upregulated hepatocyte marker genes and downregulated cholangiocyte markers (Fig. 5D), whereas Ad-c/EBPβ transduction downregulated hepatocyte markers and upregulated cholangiocyte marker genes. Promotion of hepatocyte differentiation by Ad-c/EBPα transduction was inhibited by Ad-TGFBR2 transduction, whereas inhibition of cholangiocyte differentiation by Ad-c/EBPα transduction was rescued by Ad-TGFBR2 transduction (Fig. 5E). In addition, promotion of hepatocyte differentiation by si-c/EBPβ transfection was inhibited by Ad-TGFBR2 transduction, whereas inhibition of cholangiocyte differentiation by si-c/EBPβ transfection was rescued by Ad-TGFBR2 transduction (Fig. 5F). We further confirmed that inhibition of hepatocyte differentiation by si-c/EBPα-transfection was rescued by si-TGFBR2 transfection (supplementary material Fig. S8). Taken together, these results led us to conclude that c/EBPα and c/EBPβ could determine the cell fate of HBCs by negatively and positively regulating TGFBR2 expression, respectively (supplementary material Fig. S9).

c/EBPs organize the differentiation of fetal mouse hepatoblasts through regulation of TGFBR2 expression

We have demonstrated that c/EBPs may determine the HBC fate decision via regulation of the expression level of TGFBR2. To examine whether our findings could be replicated in native liver

Development (2014) doi:10.1242/dev.103168

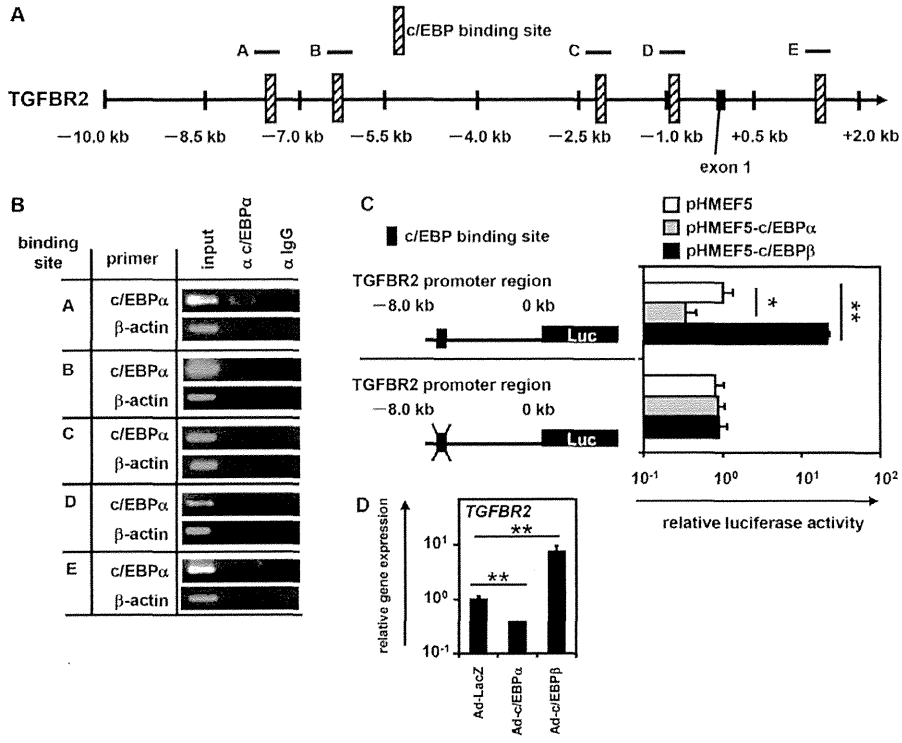

Fig. 4. *TGFBR2* promoter activity and expression are negatively regulated by c/EBPα and positively regulated by c/EBPβ. (A) Candidate c/EBP binding sites (hatched boxes) in the *TGFBR2* promoter region as predicted using rVista 2.0 (see supplementary material Fig. S7). (B) hESCs (H9 cells) were differentiated into hepatoblasts and then a ChIP assay performed. The antibodies and primers employed are summarized in supplementary material Tables S1 and S4. (C) HEK293 cells were transfected with firefly luciferase (Luc) expression plasmids containing the promoter region of *TGFBR2*. In addition, empty plasmid (pHMEF5), c/EBPα expression plasmid (pHMEF5-c/EBPα) or c/EBPβ expression plasmid (pHMEF5-c/EBPβ) was transfected. After 36 hours, a dual luciferase assay was performed. Base pair positions are relative to the translation start site (+1). (D) HepG2 cells (TGFBR2-positive cells) were transduced with 3000 VPs/cell of Ad-LacZ, Ad-c/EBPα or Ad-c/EBPβ for 1.5 hours and cultured for 48 hours. The expression level of *TGFBR2* in HepG2 cells was measured by real-time RT-PCR. On the *y*-axis, the gene expression level in Ad-LacZ-transduced cells was taken as 1.0. **P*<0.05, ***P*<0.01. Error bars indicate s.d. Statistical analysis was performed using the unpaired two-tailed Student's *t*-test (*n*=3).

development, fetal hepatoblasts were purified from E13.5 mice. The gene expression level of *TGFBR2* in fetal mouse hepatoblasts was negatively or positively regulated by c/EBPα or c/EBPβ, respectively (Fig. 6A,B). The promotion of hepatocyte differentiation by Ad-c/EBPα transduction was inhibited by Ad-TGFBR2 transduction, whereas the inhibition of cholangiocyte differentiation by Ad-c/EBPα transduction was rescued by Ad-TGFBR2 transduction (Fig. 6C). In addition, the promotion of hepatocyte differentiation by si-c/EBPβ transfection was inhibited by Ad-TGFBR2 transduction, whereas the inhibition of cholangiocyte differentiation by si-c/EBPβ transfection was rescued by Ad-TGFBR2 transduction (Fig. 6D). Taken together, these results led us to conclude that c/EBPα and c/EBPβ could determine the cell fate of fetal mouse hepatoblasts by negatively and positively regulating TGFBR2 expression, respectively. Our *in vitro* differentiation system could also prove useful in elucidating the molecular mechanisms of human liver development.

DISCUSSION

The purpose of this study was to better understand the molecular mechanisms of the hepatoblast fate decision in humans. To elucidate the molecular mechanisms of liver development, both conditional knockout mouse models and cell culture systems are useful. For example, DeLaForest et al. demonstrated the role of HNF4α in hepatocyte differentiation using hESC culture systems (DeLaForest et al., 2011). The technology for inducing hepatocyte differentiation from hESCs has recently been dramatically advanced (Takayama et al., 2012a). Because it is possible to generate functional HBCs from hESCs, which can self-replicate and differentiate into both hepatocyte and cholangiocyte lineages (supplementary material Fig. S1 and Fig. 1), the differentiation model of HBCs generated from hESCs should provide a powerful tool for analyzing the molecular mechanisms of human liver development.

In this study, the molecular mechanisms of the hepatoblast fate decision were elucidated using hESC culture systems. HBCs cultured on human LN111 expressed hepatoblast markers (supplementary material Fig. S1) and had the ability to differentiate into both hepatocyte-like cells and cholangiocyte-like cells (Fig. 1). Because a previous study showed that low and high concentrations of TGFβ were required for hepatocyte and cholangiocyte differentiation, respectively (Clotman et al., 2005), we expected that TGFBR2 might contribute to the hepatoblast fate decision. Although TGFβ1, β2 and β3 are all ligands of TGFBR2, TGFβ3 did not promote cholangiocyte differentiation (Fig. 2). This might have been because only TGFβ3 is unable to upregulate the expression of *SOX9*, which is the key factor in bile duct development *in vivo* and cholangiocyte differentiation *in vitro* (Antoniou et al., 2009). We examined the function of TGFBR2 in the hepatoblast fate decision, and found that its overexpression promoted cholangiocyte differentiation, whereas TGFBR2 knockdown promoted hepatocyte differentiation (Fig. 3). Although an exogenous TGFβ ligand was not added to the differentiation medium, the endogenous TGFβ ligand present in Matrigel, which was used in our differentiation protocol, might have bound to TGFBR2. It might also be that the cells committed to the biliary lineage express TGFβ, as a previous study showed that bile duct epithelial cells express TGFβ (Lewindon et al., 2002).

To examine the molecular mechanism regulating TGFBR2 expression, the *TGFBR2* promoter region was analyzed (Fig. 4). *TGFBR2* promoter activity was negatively regulated by c/EBPα and positively regulated by c/EBPβ. c/EBPα overexpression downregulated *TGFBR2* promoter activity in spite of the fact that c/EBPα protein has no repression domain (Yoshida et al., 2006). CTBP1 and CTBP2 (Vernochet et al., 2009) are known to be co-repressors of c/EBPα, and as such constitute candidate co-repressors recruited to the c/EBP binding site in the *TGFBR2* promoter region.

Development (2014) doi:10.1242/dev.103168

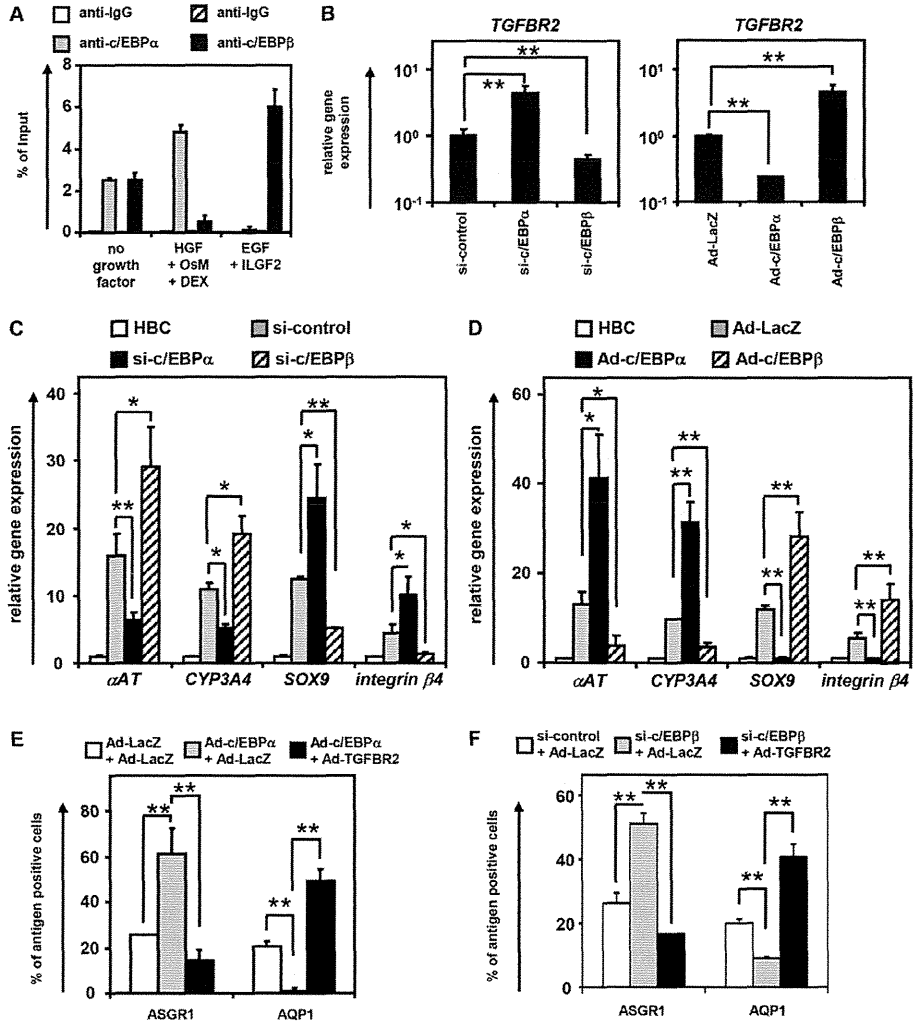

Fig. 5. c/EBPα and c/EBPβ promote hepatocyte and cholangiocyte differentiation by regulating *TGFBR2* expression, respectively. (A) HBCs were differentiated into hepatocyte-like cells or cholangiocyte-like cells according to the scheme outlined in Fig. 1A. On day 10 after hepatocyte or cholangiocyte differentiation, recruitment of c/EBPα or c/EBPβ to the *TGFBR2* promoter region was examined by ChIP assay. (B-D) HBCs were transfected with 50 nM si-control, si-c/EBPα or si-c/EBPβ and cultured in differentiation hESF-DIF medium for 10 days (B left, C). The expression levels of *TGFBR2* and hepatocyte and cholangiocyte markers were then measured by real-time RT-PCR. (B right, D) HBCs were transduced with 3000 VPs/cell of Ad-LacZ, Ad-c/EBPα or Ad-c/EBPβ for 1.5 hours and cultured in differentiation hESF-DIF medium for 10 days. The expression levels of *TGFBR2* and hepatocyte and cholangiocyte markers were then measured by real-time RT-PCR. On the *y*-axis, the gene expression level in the si-control-transfected or Ad-LacZ-transduced cells was taken as 1.0 in B, and levels in HBCs were taken as 1.0 in C and D. (E) HBCs were transduced with 3000 VPs/cell each of Ad-LacZ + Ad-LacZ, Ad-c/EBPα + Ad-LacZ, or Ad-c/EBPα + Ad-TGFBR2 for 1.5 hours and cultured in differentiation hESF-DIF medium for 10 days. The efficiency of hepatocyte or cholangiocyte differentiation was measured by estimating the percentage of ASGR1-positive or AQP1-positive cells, respectively, by FACS analysis. (F) HBCs were transduced with 3000 VPs/cell of Ad-LacZ or Ad-TGFBR2 and then transfected with 50 nM si-control or si-c/EBPβ and cultured in hESF-DIF medium for 10 days. The efficiency of hepatocyte or cholangiocyte differentiation was measured by estimating the percentage of ASGR1-positive or AQP1-positive cells, respectively, by FACS analysis. **P*<0.05, ***P*<0.01. Error bars indicate s.d. Statistical analysis was performed using the unpaired two-tailed Student's *t*-test (*n*=3).

Proteome analysis of c/EBPα would provide an opportunity to identify the co-repressor of c/EBPα. Because large numbers of nearly homogeneous hepatoblasts can be differentiated from hESCs, as compared with the isolation of fetal liver hepatoblasts, hepatocyte differentiation technology from hESCs might prove useful in proteome analysis.

We found that Ad-c/EBPα transduction could promote hepatocyte differentiation by suppressing TGFBR2 expression (Fig. 5). Our findings might thus provide a detailed explanation of the phenotype of *c/EBPα* knockout mice; that is, hepatocyte differentiation is inhibited and cholangiocyte differentiation is promoted in these mice (Yamasaki et al., 2006). We also found that Ad-c/EBPβ transduction could promote cholangiocyte differentiation by enhancing TGFBR2 expression. Because both c/EBPα and c/EBPβ can bind to the same binding site, reciprocal competition for binding is likely to be influenced by regulating c/EBPα or c/EBPβ expression. Therefore, the expression ratio between c/EBPα and c/EBPβ might determine the cell fate of hepatoblasts by regulating the expression level of TGFBR2. We confirmed that our findings could be reproduced in fetal mouse hepatoblasts (Fig. 6). Because a previous study had

Development (2014) doi:10.1242/dev.103168

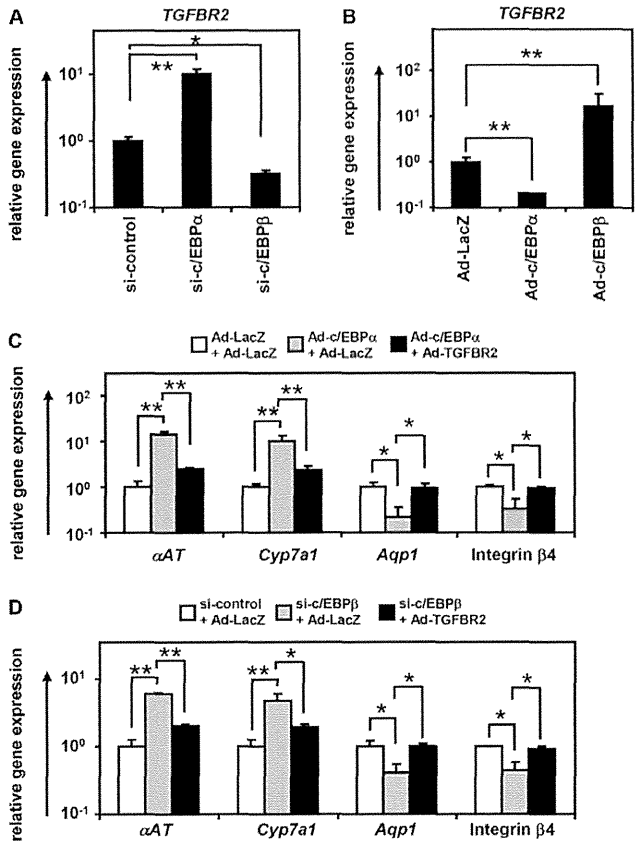

Fig. 6. c/EBPs control the differentiation of fetal mouse hepatoblasts through regulation of TGFBR2 expression. Fetal mouse hepatoblasts (Dlk1-positive cells; the purity was over 98%) were sorted from E13.5 mouse liver. (A) Fetal mouse hepatoblasts were transfected with 50 nM si-control, si-c/EBPα or si-c/EBPβ and cultured for 5 days. The expression of *TGFBR2* was measured by real-time RT-PCR. (B) Fetal mouse hepatoblasts were transduced with 3000 VPs/cell of Ad-LacZ, Ad-c/EBPα or Ad-c/EBPβ for 1.5 hours and cultured for 5 days. The expression of *TGFBR2* was measured by real-time RT-PCR. On the *y*-axis, the gene expression level in the si-control-transfected cells or Ad-LacZ-transduced cells was taken as 1.0. (C) Fetal mouse hepatoblasts were transduced with 3000 VPs/cell each of Ad-LacZ + Ad-LacZ, Ad-c/EBPα + Ad-LacZ, or Ad-c/EBPα + Ad-TGFBR2 for 1.5 hours and cultured for 5 days. On day 5, the expression levels of hepatocyte (*αAT* and *Cyp7a1*) and cholangiocyte (*Aqp1* and integrin β4) markers were measured by real-time RT-PCR. (D) Fetal mouse hepatoblasts were transduced with 3000 VPs/cell of Ad-LacZ or Ad-TGFBR2 and then transfected with 50 nM si-control or si-c/EBPβ and cultured for 5 days. On day 5, the gene levels of hepatocyte (*αAT* and *Cyp7a1*) and cholangiocyte (*Aqp1* and integrin β4) markers were measured by real-time RT-PCR. On the *y*-axis, the gene expression level in the si-control-transfected or Ad-LacZ-transduced cells was taken as 1.0. **P*<0.05, ***P*<0.01. Error bars indicate s.d. Statistical analysis was performed using the unpaired two-tailed Student's *t*-test (*n*=3).

shown that the addition of hepatocyte growth factor (HGF) to hepatoblasts upregulated the expression of c/EBPα and downregulated the expression of c/EBPβ (Suzuki et al., 2003), the ratio between c/EBPα and c/EBPβ might be determined by HGF during hepatocyte differentiation.

In this study, we have identified for the first time that *TGFBR2* is a target of c/EBPs in the hepatoblast fate decision (supplementary material Fig. S9). c/EBPα promotes hepatocyte differentiation by downregulating the expression of TGFBR2, whereas c/EBPβ promotes cholangiocyte differentiation by upregulating TGFBR2 expression. This study might have revealed a molecular mechanism underlying the lineage commitment of human hepatoblasts controlled by a gradient of TGFβ signaling. We believe that similar procedures that adopt the model of human pluripotent stem cell (including human iPS cell) differentiation will be used not only for the elucidation of molecular mechanisms underlying human hepatocyte and biliary differentiation but also for investigating the causes of congenital anomalies of the human liver and biliary tract.

MATERIALS AND METHODS

Ad vectors

Ad vectors were constructed by an improved *in vitro* ligation method (Mizuguchi and Kay, 1998; Mizuguchi and Kay, 1999). The human *c/EBPα* and *c/EBPβ* genes (accession numbers NM_004364 and NM_005194, respectively) were amplified by PCR using the following primers: c/EBPα, Fwd 5′-GCTCTAGATGCCGGGAGAACTCTAACTC-3′ and Rev 5′-GCGGTACCAAACCACTCCCTGGGTCC-3′; c/EBPβ, Fwd 5′-GCATCTAGATTCATGCAACGCCTGGTG-3′ and Rev 5′-ATAGGTACCTAAAATTACCGACGGGCTCC-3′. The human *TGFBR2* gene was purchased from Addgene (plasmid 16622). The human *c/EBPα*, *c/EBPβ* or *TGFBR2* gene was inserted into pBSKII (Invitrogen), resulting in pBSKII-c/EBPα, -c/EBPβ or -TGFBR2. Then, human *c/EBPα*, *c/EBPβ* or *TGFBR2* was inserted into pHMEF5 (Kawabata et al., 2005), which contains the human elongation factor 1α (*EF1α*, also known as *EEF1A1*) promoter, resulting in pHMEF5-c/EBPα, -c/EBPβ or -TGFBR2. pHMEF5-c/EBPα, -c/EBPβ or -TGFBR2 was digested with I-*Ceu*I/PI-*Sce*I and ligated into I-*Ceu*I/PI-*Sce*I-digested pAdHM41-K7 (Koizumi et al., 2003), resulting in pAd-c/EBPα, -c/EBPβ or -TGFBR2. The human *EF1α* promoter-driven *lacZ*- or FOXA2-expressing Ad vectors (Ad-LacZ or Ad-FOXA2, respectively) were constructed previously (Takayama et al., 2012b; Tashiro et al., 2008). All Ad vectors contain a stretch of lysine residues (K7) in the C-terminal region of the fiber knob for more efficient transduction of hESCs, definitive endoderm cells and HBCs, in which transfection efficiency was almost 100%, and the Ad vectors were purified as described previously (Takayama et al., 2012a; Takayama et al., 2011). The vector particle (VP) titer was determined by a spectrophotometric method (Maizel et al., 1968).

hESC culture

The H9 hESC line (WiCell Research Institute) was maintained on a feeder layer of mitomycin C-treated mouse embryonic fibroblasts (Merck Millipore) in ReproStem medium (ReproCELL) supplemented with 5 ng/ml FGF2 (Katayama Kagaku Kogyo). H9 was used following the Guidelines for Derivation and Utilization of Human Embryonic Stem Cells of the Ministry of Education, Culture, Sports, Science and Technology of Japan and the study was approved by the Independent Ethics Committee.

Generation and maintenance of hESC-derived HBCs

Before the initiation of cellular differentiation, the hESC medium was exchanged for a defined serum-free medium, hESF9, and cultured as previously reported (Furue et al., 2008). The differentiation protocol for the induction of definitive endoderm cells and HBCs was based on our previous reports with some modifications (Takayama et al., 2012a; Takayama et al., 2012b; Takayama et al., 2011). Briefly, in mesendoderm differentiation, hESCs were cultured for 2 days on Matrigel Matrix (BD Biosciences) in differentiation hESF-DIF medium, which contains 100 ng/ml activin A (R&D Systems); hESF-DIF medium was purchased from Cell Science & Technology Institute; differentiation hESF-DIF medium was supplemented with 10 μg/ml human recombinant insulin, 5 μg/ml human apotransferrin, 10 μM 2-mercaptoethanol, 10 μM ethanolamine, 10 μM sodium selenite, 0.5 mg/ml bovine fatty acid-free serum albumin (all from Sigma) and 1× B27 Supplement (without vitamin A; Invitrogen). To generate definitive endoderm cells, the mesendoderm cells were transduced with 3000 VPs/cell of FOXA2-expressing Ad vector (Ad-FOXA2) for 1.5 hours on day 2 and cultured until day 6 on Matrigel in differentiation hESF-DIF medium supplemented with 100 ng/ml activin A. For induction of the HBCs, the

definitive endoderm cells were cultured for 3 days on Matrigel in differentiation hESF-DIF medium supplemented with 20 ng/ml BMP4 (R&D Systems) and 20 ng/ml FGF4 (R&D Systems). Transient overexpression of FOXA2 in the mesendoderm cells is not necessary for establishing HBCs, but it is helpful for efficient generation of the HBCs. The HBCs were first purified from the hESC-derived cells (day 9) by selecting attached cells on a human recombinant LN111 (BioLamina)-coated dish 15 minutes after plating (Takayama et al., 2013). The HBCs were cultured on a human LN111-coated dish (2.0×10^4 cells/cm^2) in maintenance DMEM/F12 medium [DMEM/F12 medium (Invitrogen) supplemented with 10% fetal bovine serum (FBS), 1× insulin/transferrin/selenium, 10 mM nicotinamide, 0.1 μM dexamethasone (DEX) (Sigma), 20 mM HEPES, 25 mM $NaHCO_3$, 2 mM L-glutamine, and penicillin/streptomycin] which contained 40 ng/ml HGF (R&D Systems) and 20 ng/ml epidermal growth factors (EGF) (R&D Systems). The medium was refreshed every day. The HBCs were dissociated with Accutase (Millipore) into single cells, and subcultured every 6 or 7 days. The HBCs used in this study were passaged more than three times.

In vitro hepatocyte and cholangiocyte differentiation

To induce hepatocyte differentiation, the HBCs were cultured on a Matrigel-coated dish (7.5×10^4 cells/cm^2) in Hepatocyte Culture Medium (HCM without EGF; Lonza) supplemented with 20 ng/ml HGF, 20 ng/ml Oncostatin M (OsM) (R&D Systems) and 1 μM DEX. To induce cholangiocyte differentiation, the HBCs were cultured in collagen gel. To establish collagen gel plates, 500 μl collagen gel solution [400 μl type I-A collagen (Nitta gelatin), 50 μl 10× DMEM and 50 μl 200 mM HEPES buffer containing 2.2% $NaHCO_3$ and 0.05 M NaOH] was added to each well, and then the plates were incubated at 37°C for 30 minutes. The HBCs (5×10^4 cells) were resuspended in 500 μl differentiation DMEM/F12 medium [DMEM/F12 medium supplemented with 20 mM HEPES, 2 mM L-glutamine, 100 ng/ml EGF and 40 ng/ml ILGF2 (IGF2)], and then mixed with 500 μl of the collagen gel solution and plated onto the basal layer of collagen. After 30 minutes, 2 ml differentiation DMEM/F12 medium was added to the well.

Inhibition of TGFβ signaling

SB-431542 (Santa Cruz Biotechnology), which is a small molecule that acts as a selective inhibitor of activin receptor-like kinase (ALK) receptors [ALK4, ALK5 and ALK7 (also known as ACVR1B, TGFBR1 and ACVR1C)], was used to inhibit TGFβ signaling in HBCs.

Flow cytometry

Single-cell suspensions of hESC-derived cells were fixed with 2% paraformaldehyde (PFA) at 4°C for 20 minutes, and then incubated with primary antibody (supplementary material Table S1) followed by secondary antibody (supplementary material Table S2). Flow cytometry analysis was performed using a FACS LSR Fortessa flow cytometer (BD Biosciences). Cell sorting was performed using a FACS Aria (BD Biosciences).

RNA isolation and reverse transcription (RT)-PCR

Total RNA was isolated from hESCs and their derivatives using ISOGENE (Nippon Gene). cDNA was synthesized using 500 ng total RNA with the SuperScript VILO cDNA Synthesis Kit (Invitrogen). Real-time RT-PCR was performed with SYBR Green PCR Master Mix (Applied Biosystems) using an Applied Biosystems StemOnePlus real-time PCR system. Relative quantification was performed against a standard curve and the values were normalized against the input determined for the housekeeping gene *GAPDH*. Primers are described in supplementary material Table S3.

Immunohistochemistry

Cells were fixed with 4% PFA. After incubation with 0.1% Triton X-100 (Wako), blocking with Blocking One (Nakalai Tesque) or PBS containing 2% FBS, 2% BSA and 0.1% Triton X-100, the cells were incubated with primary antibody (supplementary material Table S1) at 4°C overnight, followed by secondary antibody (supplementary material Table S2) at room temperature for 1 hour. Immunopositive cells were counted in at least eight randomly chosen fields.

HBC colony formation assay

For the colony formation assay, HBCs were cultured at a low density (200 cells/cm^2) on a human LN111-coated dish in maintenance DMEM/F12 medium supplemented with 25 μM LY-27632 (ROCK inhibitor; Millipore).

Transplantation of clonally derived HBCs

Clonally derived HBCs were dissociated using Accutase and then suspended in maintenance DMEM/F12 medium without serum. The HBCs (1×10^6 cells) were transplanted 24 hours after administration of CCl_4 (2 mg/kg) by intrasplenic injection into 8- to 10-week-old *Rag2/Il2rg* double-knockout mice. Recipient mouse livers and blood were harvested 2 weeks after transplantation. Grafts were fixed with 4% PFA and processed for immunohistochemistry. Serum was extracted and subjected to ELISA. All animal experiments were conducted in accordance with institutional guidelines.

ELISA

Levels of human ALB in mouse serum were examined by ELISA using kits from Bethyl Laboratories according to the manufacturer's instructions.

Culture of mouse Dlk1$^+$ cells

Dlk1$^+$ hepatoblasts were isolated from E13.5 mouse livers using anti-mouse Dlk1 monoclonal antibody (MBL International Corporation, D187-4) as described previously (Tanimizu et al., 2003). Dlk1$^+$ cells were resuspended in DMEM/F12 (Sigma) containing 10% FBS, 1× insulin/transferrin/selenium (ITS), 10 mM nicotinamide (Wako), 0.1 μM DEX and 5 mM L-glutamine. Cells were plated on laminin-coated dishes and cultured in medium containing 20 ng/ml HGF, EGF and 25 μM LY-27632 (ROCK inhibitor).

lacZ assay

Hepatoblasts were transduced with Ad-LacZ at 3000 VPs/cell for 1.5 hours. The day after transduction (day 10), 5-bromo-4-chloro-3-indolyl β-D-galactopyranoside (X-Gal) staining was performed as described previously (Kawabata et al., 2005).

Reporter assays

The effects of c/EBPα or c/EBPβ overexpression on *TGFBR2* promoter activity were examined using a reporter assay. An 8 kb fragment of the 5′ flanking region of the *TGFBR2* gene was amplified by PCR using the following primers: Fwd, 5′-CCGAGCTCATGTTTGATGAAGTGTCTAG-CTTCCAAGG-3′; Rev, 5′-GGCTCGAGCCTCGACGTCCAGCCCCT-3′. The fragment was inserted into the *Sac*I/*Xho*I sites of pGL3-basic (Promega), resulting in a pGL3-*TGFBR2* promoter region (pGL3-TGFBR2-PR). To generate a *TGFBR2* promoter region containing mutations in the c/EBP binding site, the following primers were used in PCR (mutations are indicated by lowercase letters): Fwd, 5′-CACTAGTATTCAgTG-AtCcgAAAATATGG-3′; Rev, 5′-CACTAGTATTCAgTGAtCcgAAAA-TATGG-3′; this resulted in pGL3-mTGFBR2-PR. HEK293 cells were maintained in DMEM (Wako) supplemented with 10% FBS, penicillin and streptomycin, and 2 mM L-glutamine. In reporter assays, 60 ng pGL3-TGFBR2-PR or pGL3-mTGFBR2-PR was transfected together with 720 ng each expression plasmid (pHMEF5, pHMEF5-c/EBPα and pHMEF5-c/EBPβ) and 60 ng internal control plasmid (pCMV-Renilla luciferase) using Lipofectamine 2000 reagent (Invitrogen). Transfected cells were cultured for 36 hours, and a Dual Luciferase Assay (Promega) was performed according to the manufacturer's instructions.

siRNA-mediated knockdown

Predesigned siRNAs targeting *c/EBPα*, *c/EBPβ* and *TGFBR2* mRNAs were purchased from Thermo Scientific Dharmacon. Cells were transfected with 50 nM siRNA using RNAiMAX (Invitrogen) transfection reagent according to the manufacturer's instructions. As a negative control, we used scrambled siRNA (Qiagen) of a sequence showing no significant similarity to any mammalian gene.

Chromatin immunoprecipitation (ChIP) assay

The ChIP assay kit was purchased from Upstate. Cells were crosslinked using formaldehyde at a final concentration of 1% at 37°C for 10 minutes, and then genomic DNA was fragmented by sonicator. The resulting DNA-protein complexes were immunoprecipitated using the antibodies described in supplementary material Table S1 or control IgG as described in supplementary material Table S2. The precipitated DNA fragments were analyzed by real-time RT-PCR using the primers shown in supplementary material Table S4 to amplify the *TGFBR2* promoter region including the c/EBP binding sites or β-actin locus as a control. The results of quantitative ChIP analysis (Fig. 5A) were expressed as the amount of amplified *TGFBR2* promoter region relative to input DNA taken as 100%.

Statistical analysis

Statistical analysis was performed using an unpaired two-tailed Student's *t*-test. All data are represented as mean ± s.d. (n=3).

Acknowledgements

We thank Natsumi Mimura, Yasuko Hagihara and Hiroko Matsumura for excellent technical support.

Competing interests

The authors declare no competing financial interests.

Author contributions

K. Takayama, K.K. and H.M. developed the concepts or approach; K. Takayama, Y.N., K.O., H.O. and T.Y. performed experiments; K. Takayama, K.K., M.I., K. Tashiro, F.S., T.H., T.O., M.F.K. and H.M. performed data analysis; K. Takayama, K.K. and H.M. prepared or edited the manuscript prior to submission.

Funding

H.M., K.K., M.K.F. and T.H. were supported by grants from the Ministry of Health, Labor, and Welfare of Japan (MEXT). H.M. was also supported by Japan Research Foundation for Clinical Pharmacology, The Uehara Memorial Foundation. K.O. was supported by Special Coordination Funds for Promoting Science and Technology from MEXT. F.S. was supported by Program for Promotion of Fundamental Studies in Health Sciences of the National Institute of Biomedical Innovation (NIBIO). K. Takayama and Y.N. are Research Fellows of the Japan Society for the Promotion of Science.

Supplementary material

Supplementary material available online at
http://dev.biologists.org/lookup/suppl/doi:10.1242/dev.103168/-/DC1

References

Agarwal, S., Holton, K. L. and Lanza, R. (2008). Efficient differentiation of functional hepatocytes from human embryonic stem cells. *Stem Cells* **26**, 1117-1127.

Antoniou, A., Raynaud, P., Cordi, S., Zong, Y., Tronche, F., Stanger, B. Z., Jacquemin, P., Pierreux, C. E., Clotman, F. and Lemaigre, F. P. (2009). Intrahepatic bile ducts develop according to a new mode of tubulogenesis regulated by the transcription factor SOX9. *Gastroenterology* **136**, 2325-2333.

Chen, S. S., Chen, J. F., Johnson, P. F., Muppala, V. and Lee, Y. H. (2000). C/EBPbeta, when expressed from the C/ebpalpha gene locus, can functionally replace C/EBPalpha in liver but not in adipose tissue. *Mol. Cell. Biol.* **20**, 7292-7299.

Clotman, F., Jacquemin, P., Plumb-Rudewiez, N., Pierreux, C. E., Van der Smissen, P., Dietz, H. C., Courtoy, P. J., Rousseau, G. G. and Lemaigre, F. P. (2005). Control of liver cell fate decision by a gradient of TGF beta signaling modulated by Onecut transcription factors. *Genes Dev.* **19**, 1849-1854.

DeLaForest, A., Nagaoka, M., Si-Tayeb, K., Noto, F. K., Konopka, G., Battle, M. A. and Duncan, S. A. (2011). HNF4A is essential for specification of hepatic progenitors from human pluripotent stem cells. *Development* **138**, 4143-4153.

Furue, M. K., Na, J., Jackson, J. P., Okamoto, T., Jones, M., Baker, D., Hata, R., Moore, H. D., Sato, J. D. and Andrews, P. W. (2008). Heparin promotes the growth of human embryonic stem cells in a defined serum-free medium. *Proc. Natl. Acad. Sci. USA* **105**, 13409-13414.

Hansen, A. J., Lee, Y. H., Sterneck, E., Gonzalez, F. J. and Mackenzie, P. I. (1998). C/EBPalpha is a regulator of the UDP glucuronosyltransferase UGT2B1 gene. *Mol. Pharmacol.* **53**, 1027-1033.

Kawabata, K., Sakurai, F., Yamaguchi, T., Hayakawa, T. and Mizuguchi, H. (2005). Efficient gene transfer into mouse embryonic stem cells with adenovirus vectors. *Mol. Ther.* **12**, 547-554.

Kitisin, K., Saha, T., Blake, T., Golestaneh, N., Deng, M., Kim, C., Tang, Y., Shetty, K., Mishra, B. and Mishra, L. (2007). Tgf-Beta signaling in development. *Sci. STKE* **2007**, cm1.

Koizumi, N., Mizuguchi, H., Utoguchi, N., Watanabe, Y. and Hayakawa, T. (2003). Generation of fiber-modified adenovirus vectors containing heterologous peptides in both the HI loop and C terminus of the fiber knob. *J. Gene Med.* **5**, 267-276.

Lewindon, P. J., Pereira, T. N., Hoskins, A. C., Bridle, K. R., Williamson, R. M., Shepherd, R. W. and Ramm, G. A. (2002). The role of hepatic stellate cells and transforming growth factor-beta(1) in cystic fibrosis liver disease. *Am. J. Pathol.* **160**, 1705-1715.

Maizel, J. V., Jr, White, D. O. and Scharff, M. D. (1968). The polypeptides of adenovirus. I. Evidence for multiple protein components in the virion and a comparison of types 2, 7A, and 12. *Virology* **36**, 115-125.

Mizuguchi, H. and Kay, M. A. (1998). Efficient construction of a recombinant adenovirus vector by an improved in vitro ligation method. *Hum. Gene Ther.* **9**, 2577-2583.

Mizuguchi, H. and Kay, M. A. (1999). A simple method for constructing E1- and E1/E4-deleted recombinant adenoviral vectors. *Hum. Gene Ther.* **10**, 2013-2017.

Oe, S., Lemmer, E. R., Conner, E. A., Factor, V. M., Levéen, P., Larsson, J., Karlsson, S. and Thorgeirsson, S. S. (2004). Intact signaling by transforming growth factor beta is not required for termination of liver regeneration in mice. *Hepatology* **40**, 1098-1105.

Plumb-Rudewiez, N., Clotman, F., Strick-Marchand, H., Pierreux, C. E., Weiss, M. C., Rousseau, G. G. and Lemaigre, F. P. (2004). Transcription factor HNF-6/OC-1 inhibits the stimulation of the HNF-3alpha/Foxa1 gene by TGF-beta in mouse liver. *Hepatology* **40**, 1266-1274.

Schmelzer, E., Zhang, L., Bruce, A., Wauthier, E., Ludlow, J., Yao, H. L., Moss, N., Melhem, A., McClelland, R., Turner, W. et al. (2007). Human hepatic stem cells from fetal and postnatal donors. *J. Exp. Med.* **204**, 1973-1987.

Suzuki, A., Iwama, A., Miyashita, H., Nakauchi, H. and Taniguchi, H. (2003). Role for growth factors and extracellular matrix in controlling differentiation of prospectively isolated hepatic stem cells. *Development* **130**, 2513-2524.

Takayama, K., Inamura, M., Kawabata, K., Tashiro, K., Katayama, K., Sakurai, F., Hayakawa, T., Furue, M. K. and Mizuguchi, H. (2011). Efficient and directive generation of two distinct endoderm lineages from human ESCs and iPSCs by differentiation stage-specific SOX17 transduction. *PLoS ONE* **6**, e21780.

Takayama, K., Inamura, M., Kawabata, K., Katayama, K., Higuchi, M., Tashiro, K., Nonaka, A., Sakurai, F., Hayakawa, T., Furue, M. K. et al. (2012a). Efficient generation of functional hepatocytes from human embryonic stem cells and induced pluripotent stem cells by HNF4α transduction. *Mol. Ther.* **20**, 127-137.

Takayama, K., Inamura, M., Kawabata, K., Sugawara, M., Kikuchi, K., Higuchi, M., Nagamoto, Y., Watanabe, H., Tashiro, K., Sakurai, F. et al. (2012b). Generation of metabolically functioning hepatocytes from human pluripotent stem cells by FOXA2 and HNF1α transduction. *J. Hepatol.* **57**, 628-636.

Takayama, K., Nagamoto, Y., Mimura, N., Tashiro, K., Sakurai, F., Tachibana, M., Hayakawa, T., Kawabata, K. and Mizuguchi, H. (2013). Long-term self-renewal of human ES/iPS-derived hepatoblast-like cells on human laminin 111-coated dishes. *Stem Cell Reports* **1**, 322-335.

Tanimizu, N., Nishikawa, M., Saito, H., Tsujimura, T. and Miyajima, A. (2003). Isolation of hepatoblasts based on the expression of Dlk/Pref-1. *J. Cell Sci.* **116**, 1775-1786.

Tashiro, K., Kawabata, K., Sakurai, H., Kurachi, S., Sakurai, F., Yamanishi, K. and Mizuguchi, H. (2008). Efficient adenovirus vector-mediated PPAR gamma gene transfer into mouse embryoid bodies promotes adipocyte differentiation. *J. Gene Med.* **10**, 498-507.

Tomizawa, M., Garfield, S., Factor, V. and Xanthopoulos, K. G. (1998). Hepatocytes deficient in CCAAT/enhancer binding protein alpha (C/EBP alpha) exhibit both hepatocyte and biliary epithelial cell character. *Biochem. Biophys. Res. Commun.* **249**, 1-5.

Vernochet, C., Peres, S. B., Davis, K. E., McDonald, M. E., Qiang, L., Wang, H., Scherer, P. E. and Farmer, S. R. (2009). C/EBPalpha and the corepressors CtBP1 and CtBP2 regulate repression of select visceral white adipose genes during induction of the brown phenotype in white adipocytes by peroxisome proliferator-activated receptor gamma agonists. *Mol. Cell. Biol.* **29**, 4714-4728.

Yamasaki, H., Sada, A., Iwata, T., Niwa, T., Tomizawa, M., Xanthopoulos, K. G., Koike, T. and Shiojiri, N. (2006). Suppression of C/EBPalpha expression in periportal hepatoblasts may stimulate biliary cell differentiation through increased Hnf6 and Hnf1b expression. *Development* **133**, 4233-4243.

Yoshida, Y., Hughes, D. E., Rausa, F. M., III, Kim, I. M., Tan, Y., Darlington, G. J. and Costa, R. H. (2006). C/EBPalpha and HNF6 protein complex formation stimulates HNF6-dependent transcription by CBP coactivator recruitment in HepG2 cells. *Hepatology* **43**, 276-286.

BNIP3 Plays Crucial Roles in the Differentiation and Maintenance of Epidermal Keratinocytes

Mariko Moriyama[1,2,4], Hiroyuki Moriyama[1,4], Junki Uda[1], Akifumi Matsuyama[2], Masatake Osawa[3] and Takao Hayakawa[1]

Transcriptome analysis of the epidermis of *Hes1*$^{-/-}$ mouse revealed the direct relationship between Hes1 (hairy and enhancer of split-1) and BNIP3 (BCL2 and adenovirus E1B 19-kDa-interacting protein 3), a potent inducer of autophagy. Keratinocyte differentiation is going along with activation of lysosomal enzymes and organelle clearance, expecting the contribution of autophagy in this process. We found that BNIP3 was expressed in the suprabasal layer of the epidermis, where autophagosome formation is normally observed. Forced expression of BNIP3 in human primary epidermal keratinocytes (HPEKs) resulted in autophagy induction and keratinocyte differentiation, whereas knockdown of BNIP3 had the opposite effect. Intriguingly, addition of an autophagy inhibitor significantly suppressed the BNIP3-stimulated differentiation of keratinocytes, suggesting that BNIP3 plays a crucial role in keratinocyte differentiation by inducing autophagy. Furthermore, the number of dead cells increased in the human epidermal equivalent of BNIP3 knockdown keratinocytes, which suggests that BNIP3 is important for maintenance of skin epidermis. Interestingly, although UVB irradiation stimulated BNIP3 expression and cleavage of caspase3, suppression of UVB-induced BNIP3 expression led to further increase in cleaved caspase3 levels. This suggests that BNIP3 has a protective effect against UVB-induced apoptosis in keratinocytes. Overall, our data provide valuable insights into the role of BNIP3 in the differentiation and maintenance of epidermal keratinocytes.

Journal of Investigative Dermatology (2014) **134,** 1627–1635; doi:10.1038/jid.2014.11; published online 6 February 2014

INTRODUCTION

The skin epidermis is a stratified epithelium. Stratification is a key process of epidermal development. During epidermal development, the single layer of basal cells undergoes asymmetric cell division to stratify, and produce committed suprabasal cells on the basal layer. These suprabasal cells are still immature and sustain several rounds of cell divisions to form fully stratified epithelia. Recent studies have identified numerous molecules involved in epidermal development, although how these molecules coordinate to induce proper stratification of the epidermis remains to be elucidated. Previously, by integrating both loss- and gain-of-function studies of Notch receptors and their downstream target Hes1 (hairy and enhancer of split-1), we demonstrated the multiple roles of Notch signaling in the regulation of suprabasal cells (Moriyama *et al.*, 2008). Notch signaling induces differentiation of suprabasal cells in a Hes1-independent manner, whereas Hes1 is required for maintenance of the immature status of suprabasal cells by preventing premature differentiation. In light of the critical role of Hes1 in the maintenance of spinous cells, exploration of the molecular targets of Hes1 in spinous layer cells may lead to the discovery of the molecules required for differentiation of spinous layer cells to granular layer cells. Because Hes1 is thought to be a transcriptional repressor (Ohtsuka *et al.*, 1999), loss of Hes1 is expected to cause aberrant upregulation of genes that are normally repressed in spinous layer cells. To identify these genes, we previously conducted comparative global transcript analysis using microarrays and found several candidates that may play a crucial role in regulating epidermal development (Moriyama *et al.*, 2008). One of the genes that was highly expressed was *BNIP3 (BCL2 and adenovirus E1B 19-kDa-interacting protein 3)*, an atypical pro-apoptotic BH3-only protein that induces cell death and autophagy (Zhang and Ney, 2009).

The molecular mechanism through which BNIP3 induces cell death is not well understood; however, it has been reported that BNIP3 protein is induced by hypoxia in some tumor cells and that the kinetics of this induction correlate with cell death (Sowter *et al.*, 2001). In contrast,

[1]*Pharmaceutical Research and Technology Institute, Kinki University, Higashi-Osaka, Osaka, Japan;* [2]*Platform for Realization of Regenerative Medicine, Foundation for Biomedical Research and Innovation, Kobe, Hyogo, Japan and* [3]*Division of Regeneration Technology, Gifu University School of Medicine, Gifu, Gifu, Japan*

[4]*These authors contributed equally to this work.*

Correspondence: Mariko Moriyama, Pharmaceutical Research and Technology Institute, Kinki University, Higashi-Osaka, Osaka 577-8502, Japan. E-mail: mariko@phar.kindai.ac.jp

Abbreviations: 3-MA, 3-methyladenine; BNIP3, BCL2 and adenovirus E1B 19-kDa-interacting protein 3; ChIP, chromatin immunoprecipitation; Hes1, hairy and enhancer of split-1; HPEK, human primary epidermal keratinocyte; Q-PCR, quantitative PCR

Received 18 July 2013; revised 10 December 2013; accepted 18 December 2013; accepted article preview online 8 January 2014; published online 6 February 2014

BNIP3-induced autophagy has been shown to protect HL-1 myocytes from cell death in an ischemia–reperfusion model (Hamacher-Brady *et al.*, 2007). Induction of autophagy by BNIP3 has a protective effect in some conditions, whereas in others it is associated with autophagic cell death. Recent evidence also suggests that BNIP3, through autophagy, is also required for the differentiation of chondrocytes under hypoxic conditions (Zhao *et al.*, 2012).

Autophagy was initially described based on its ultrastructural features of the double-membraned structures that surrounded the cytoplasm and organelles in cells, known as autophagosomes (Mizushima *et al.*, 2010). To date, only microtubule-associated protein light chain 3 (LC3), a mammalian homolog of yeast Atg8, is known to be expressed in autophagosomes and, therefore, it serves as a widely used marker for autophagosomes (Kabeya *et al.*, 2000; Mizushima *et al.*, 2004). Autophagy is an evolutionarily conserved catabolic program that is activated in response to starvation or changing nutrient conditions. Recently, autophagy was shown to be involved in differentiation of multiple cell types, including erythrocytes, lymphocytes, adipocyte, neuron, and chondrocyte (Srinivas *et al.*, 2009; Mizushima and Levine, 2010).

Epidermal cornification, the process of terminal keratinocyte differentiation, requires programmed cell death in a similar but different pathway from apoptosis (Lippens *et al.*, 2005). Cornification is also accompanied by activation of lysosomal enzymes and organelle clearance. Moreover, some researchers have reported that autophagy may play a role in epidermal differentiation (Haruna *et al.*, 2008; Aymard *et al.*, 2011; Chatterjea *et al.*, 2011). Therefore, it is likely that BNIP3 is involved in cornification through cell death or autophagy.

In this study, transcriptome analysis of *Hes1*$^{-/-}$ mouse epidermis revealed that Hes1 could directly suppress BNIP3 expression in epidermal keratinocytes. We also found that BNIP3 was expressed in the suprabasal layer of the human skin epidermis, where autophagosome formation was observed. BNIP3 was also sufficient to promote cornification through induction of autophagy. Finally, we found that BNIP3 had a protective effect against UVB-induced apoptosis in keratinocytes *in vitro*. Our data thus indicate that BNIP3, an inducer of autophagy, is involved in the terminal differentiation and maintenance of epidermal keratinocytes.

RESULTS

Hes1 directly represses BNIP3 expression in epidermal cells and keratinocytes

We previously performed a microarray analysis with epidermal RNAs isolated from wild-type and *Hes1*$^{-/-}$ mice (Moriyama *et al.*, 2008) and found that BNIP3 was preferentially overexpressed in *Hes1*$^{-/-}$ epidermis. The upregulation of *Bnip3* in the *Hes1*$^{-/-}$ epidermis was confirmed by quantitative PCR (Q-PCR) and immunofluorescent staining (Figure 1a and b). As Hes1 is thought to be a transcriptional repressor (Ishibashi *et al.*, 1994), it might play a repressive role in the regulation of BNIP3 expression. In accordance with this hypothesis, BNIP3 expression in *Hes1*$^{-/-}$ epidermis at embryonic day 15.5 was observed in the suprabasal layers (Figure 1b), where Hes1 has been reported to be expressed in wild-type epidermis at the same age (Blanpain *et al.*, 2006; Moriyama *et al.*, 2008). To confirm whether Hes1 suppresses BNIP3 expression, an adenoviral vector expressing Hes1 was used to infect human primary epidermal keratinocytes (HPEKs) and, subsequently, the expression level of BNIP3 was quantified by Q-PCR and western blot analysis. The BNIP3 protein was detected as multiple bands between 22 and 30 kD as previously reported (Vengellur and LaPres, 2004; Walls *et al.*, 2009; Mellor *et al.*, 2010; Sassone *et al.*, 2010). We found that Hes1 induced a substantial reduction of BNIP3 expression in HPEKs at the mRNA and protein levels (Figure 1c and d), demonstrating that Hes1 is involved in the repression of BNIP3. To determine whether Hes1 directly regulates *BNIP3* expression, we performed chromatin immunoprecipitation (ChIP) assays. We identified at least 5 Hes1 consensus binding sites 1 kb upstream of the transcription initiation site of the human *BNIP3* gene, and subsequent Q-PCR analysis revealed that a DNA fragment located at −247 to −87 was slightly amplified from crosslinked chromatin isolated by Hes1 immunoprecipitation (Figure 1e). We also found an additional site between −212 and +22 that was strongly amplified. These data clearly show that Hes1 specifically binds to the promoter region of *BNIP3* and directly suppresses its expression.

BNIP3 is expressed in the granular layer of the epidermis, where autophagosome formation is observed

To determine the BNIP3 expression profile in the epidermis, we performed immunofluorescent staining in human skin epidermal equivalent. BNIP3 was expressed in the granular layer of epidermal equivalent 18 days (Figure 2a and b) or 24 days (Figure 2c and d) after exposure at the air–liquid interface. BNIP3 expression in the granular layer was also observed in the normal human skin epidermis (Figure 2g and h). Recent reports show that BNIP3 is expressed in mitochondria and that it induces autophagy (Quinsay *et al.*, 2010). In addition, some researchers have reported that autophagy may play a role in epidermal differentiation (Haruna *et al.*, 2008; Aymard *et al.*, 2011; Chatterjea *et al.*, 2011). We therefore investigated whether autophagy occurred in the epidermis, especially in the granular layers. To quantitate the level of autophagy, cytosol to membrane translocation of the autophagy marker EGFP-LC3 (Kabeya *et al.*, 2000) was monitored in a human skin equivalent model (Mizushima *et al.*, 2004). When autophagy is active, autophagosomes containing EGFP-LC3 are visible as fluorescent puncta (Kabeya *et al.*, 2000). As expected, EGFP-LC3 puncta were observed in the granular layers of the epidermal equivalent (Figure 2e). Moreover, endogenous LC3 dots were observed in the granular layers of normal human skin epidermis (Figure 2f). These data suggested that BNIP3 might be involved in the induction of autophagy in the granular layer of the epidermis.

BNIP3 is required for terminal differentiation of keratinocyte by induction of autophagy *in vitro*

To investigate the involvement of BNIP3 in the induction of autophagy, we transduced HPEKs stably expressing EGFP-LC3

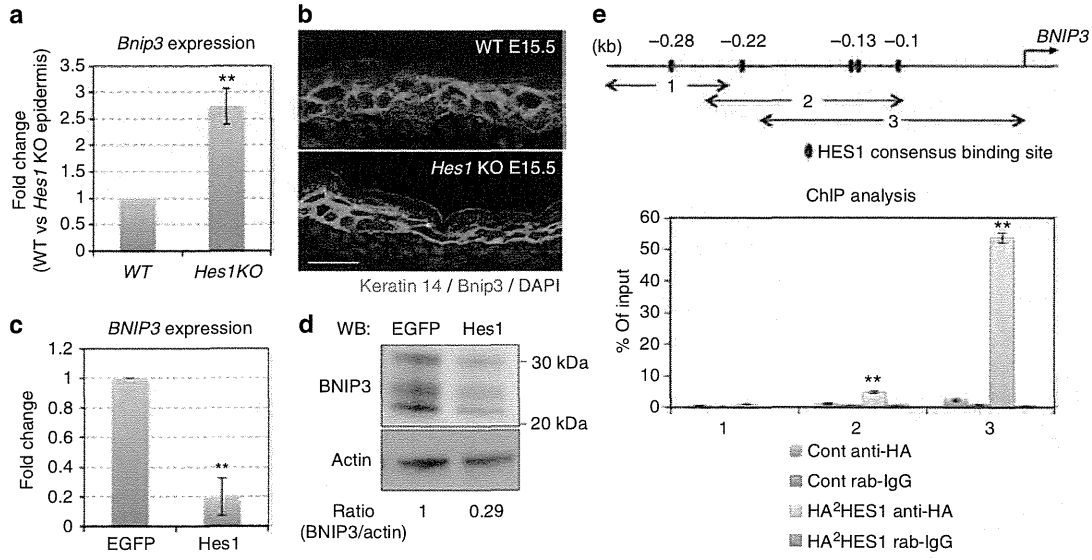

Figure 1. BNIP3 (BCL2 and adenovirus E1B 19-kDa-interacting protein 3) is directly suppressed by HES1(hairy and enhancer of split-1). (**a**) Quantitative PCR (Q-PCR) analysis of *Bnip3* expression in dorsal skin epidermis from either wild-type (WT) or *Hes1* knockout (KO) embryo (embryonic day 14.5 (E14.5)). (**b**) Immunofluorescent analysis of Bnip3 expression in dorsal skin epidermis from either WT or *Hes1* KO embryo (E15.5). Keratin 14 staining is shown in green and Bnip3 staining is shown in red. The blue signals indicate nuclear staining. Scale bars = 20 μm. (**c**) Q-PCR and (**d**) western blot analysis of BNIP3 expression in human primary epidermal keratinocyte (HPEK) cells infected with adenoviruses expressing enhanced green fluorescent protein (EGFP) or Hes1. (**c**) Each expression value was calculated with the ΔΔCt method using *UBE2D2* as an internal control. (**d**) Numbers below blots indicate relative band intensities as determined by ImageJ software. (**e**) Specific binding of Hes1 to the *BNIP3* promoter. HPEK cells were infected with adenoviral constructs expressing hemagglutinin (HA)-tagged Hes1, and processed for chromatin immunoprecipitation (ChIP) with an anti-HA antibody and normal rabbit immunoglobulin G (Cont rab-IgG) as a nonimmune control. Q-PCR amplification of the region of the *BNIP3* gene described in the indicated map (upper panel; nucleotides −360 to −244 (1); nucleotides −247 to −87 (2); −212 to +22 (3)) was also performed. The amount of precipitated DNA was calculated relative to the total input chromatin. All the data represent the average of three independent experiments ± SD. $^{**}P<0.01$.

with a BNIP3 adenoviral vector. BNIP3 expression was found to be sufficient to trigger the formation of EGFP-LC3 puncta that was significantly reduced by addition of 3-methyladenine (3-MA), an inhibitor of autophagy (Figure 3a and b). On the other hand, BNIP3 knockdown markedly decreased the punctuate distribution of EGFP-LC3 in differentiated HPEKs (Figure 3c and d). Furthermore, flow cytometry analysis using a green fluorescent probe used to specifically detect autophagy (Cyto-ID autophagy detection dye) (Chan *et al.*, 2012) also showed that BNIP3 was required for the autophagy induction (Figure 3c and f). These data indicate that BNIP3 is involved in the induction of autophagy in HPEKs. Intriguingly, these data also confirm the previous finding that autophagosome induction is accompanied by keratinocyte differentiation (Haruna *et al.*, 2008). We observed that the number of mitochondria was decreased in the granular layers, where BNIP3 expression and autophagosome formation was observed (Figure 4a). In addition, mitochondria were significantly decreased in the differentiated HPEKs *in vitro* (Figure 4b). Colocalizations of mitochondria and EGFP-LC3 dot were observed only in the differentiating keratinocytes (Figure 4c), suggesting the contribution of autophagy in the decrease of mitochondria. BNIP3 expression was also correlated with decreased mitochondria in HPEKs, whereas addition of 3-MA restored mitochondrial numbers (Figure 4d). Furthermore, we also observed colocalization of mitochondria and EGFP-LC3 dot in BNIP3-overexpressing HPEKs (Figure 4e). These data indicated that mitochondria were removed by BNIP3-induced autophagy. Next, we investigated the involvement of BNIP3 in the differentiation of epidermal keratinocytes. Western blot analysis and immunofluorescent staining revealed that BNIP3 expression increased during differentiation (Figure 5a and b). Knockdown of BNIP3 significantly suppressed keratinocyte differentiation when the cells were treated with differentiation medium (Figure 5c and d), indicating that BNIP3 is required for terminal differentiation of keratinocyte. On the other hand, forced expression of BNIP3 in HPEKs markedly stimulated loricrin expression (Figure 5e and f). To determine whether BNIP3-dependent keratinocyte differentiation was induced by autophagy, 3-MA was added to the cells transduced with BNIP3. As shown in Figure 5e and f, 3-MA notably abolished the keratinocyte differentiation induced by BNIP3, suggesting that BNIP3 is required for terminal differentiation of keratinocyte by induction of autophagy.

BNIP3 maintains epidermal keratinocytes

To further determine the roles of BNIP3 in epidermal differentiation, the human skin epidermal equivalent was reconstituted from HPEKs stably expressing a BNIP3 RNA interference (RNAi). Unfortunately, we did not observe drastic differentiation defects; however, we unexpectedly discovered

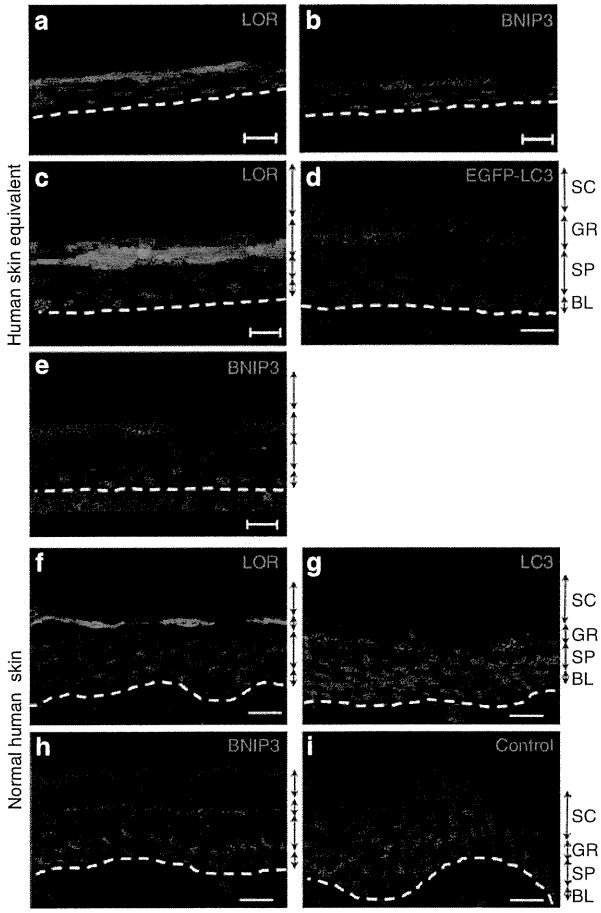

Figure 2. BNIP3 (BCL2 and adenovirus E1B 19-kDa-interacting protein 3) is expressed in the granular layer of the human epidermis. (**a–e**) Human skin epidermal equivalents were constituted from (**a–d**) normal human primary epidermal keratinocytes (HPEKs) or (**e**) HPEKs transfected with EGFP-LC3 by lentiviral vector. Cells were grown for (**a**, **b**) 18 days and (**c–e**) 24 days after exposure at the air–liquid interface. (**f–i**) Normal human skin epidermis. (**a**, **c**, **f**) Expression pattern of loricrin (LOR). (**b**, **e**, **h**) Expression pattern of BNIP3. (**i**) Control staining without BNIP3 antibody is shown. (**d**) Autophagosome formation determined by EGFP-LC3 puncta. (**g**) Endogenous expression pattern of LC3. The blue signals indicate nuclear staining. The dotted lines indicate (**a–e**) the boundary between the epidermis and the membrane or (**f–i**) the boundary between the epidermis and the dermis. Scale bars = 20 μm. BL, basal layer; GL, granular layer; SC, stratum corneum (cornified layer); SP, spinous layer.

that "sunburn-like cells" existed in BNIP3 knockdown epidermal equivalent (Figure 6a and b). We therefore hypothesized that BNIP3 might play a key role in the survival of epidermal keratinocytes. To evaluate this hypothesis, HPEKs were irradiated with 20 mJ cm^{-2} UVB. UVB irradiation triggered the formation of autophagosome that was significantly reduced by BNIP3 knockdown (Figure 6c–e). As shown in Figure 6f, UVB irradiation induced cleavage of caspase3 and BNIP3 expression. Intriguingly, knockdown of UVB-induced BNIP3 by RNAi further increased the amount of cleaved caspase3, suggesting that BNIP3 is required for the protection of keratinocytes from UVB-induced apoptosis (Figure 6f).

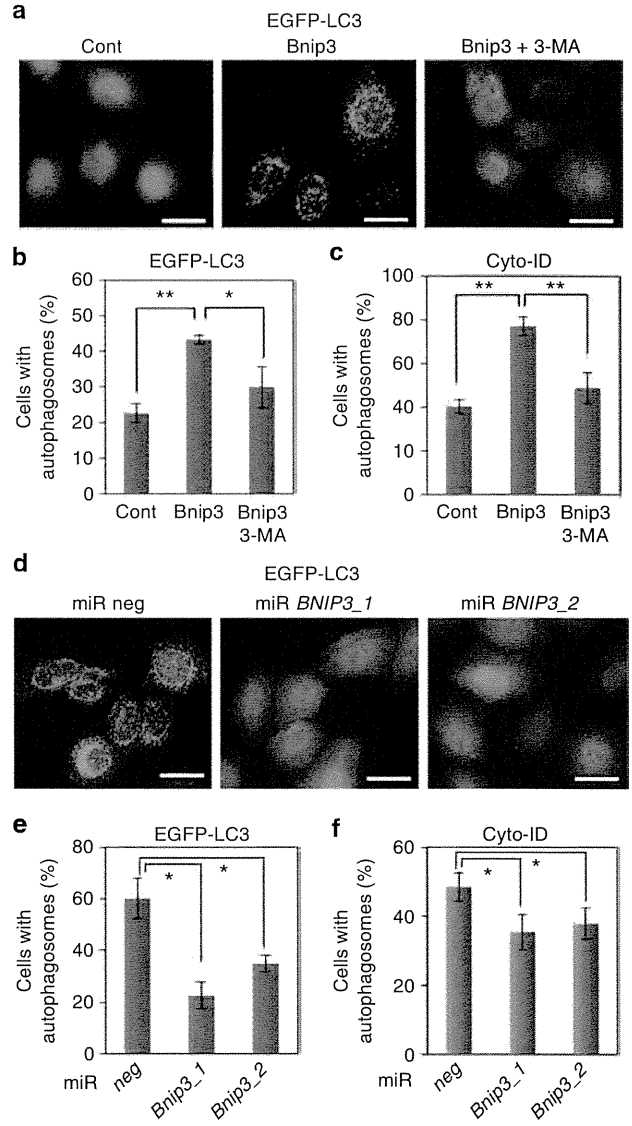

Figure 3. BNIP3 (BCL2 and adenovirus E1B 19-kDa-interacting protein 3) stimulates autophagy. (**a**, **b**) EGFP-LC3-expressing human primary epidermal keratinocytes (HPEKs) were transduced with DsRed (Cont) or BNIP3. As an inhibitor of autophagy, 3-methyladenine 3-MA (5 mM) was added. Cells were then stained with anti-EGFP at 24 hours after transduction. (**a**) EGFP-LC3 staining is shown in green. Scale bars = 20 μm. (**b**) The percentage of EGFP-LC3-positive cells with more than five puncta were quantified and are presented as the mean of three independent experiments ± SD. (**c**) HPEKs were transduced with DsRed (Cont) or BNIP3. As an inhibitor of autophagy, 3-MA (5 mM) was added. Autophagy induction was determined by Cyto-ID staining and quantified by flow cytometry. (**d**, **e**) EGFP-LC3-expressing HPEKs were transduced with miR *neg*, miR *BNIP3_1*, or miR *BNIP3_2* and induced to differentiate. Cells were then stained with anti-EGFP at 8 hours after differentiation induction. (**d**) EGFP-LC3 staining is shown in green. Scale bars = 20 μm. (**e**) The percentage of EGFP-LC3-positive cells with more than five puncta were quantified and are presented as the mean of three independent experiments ± SD. (**f**) HPEKs were transduced with miR *neg*, miR *BNIP3_1*, or miR *BNIP3_2* and induced to differentiate. Autophagy induction was determined by Cyto-ID staining and quantified by flow cytometry. All the data represent the average of three independent experiments ± SD. $^{**}P<0.01$; $^{*}0.01<P<0.05$.

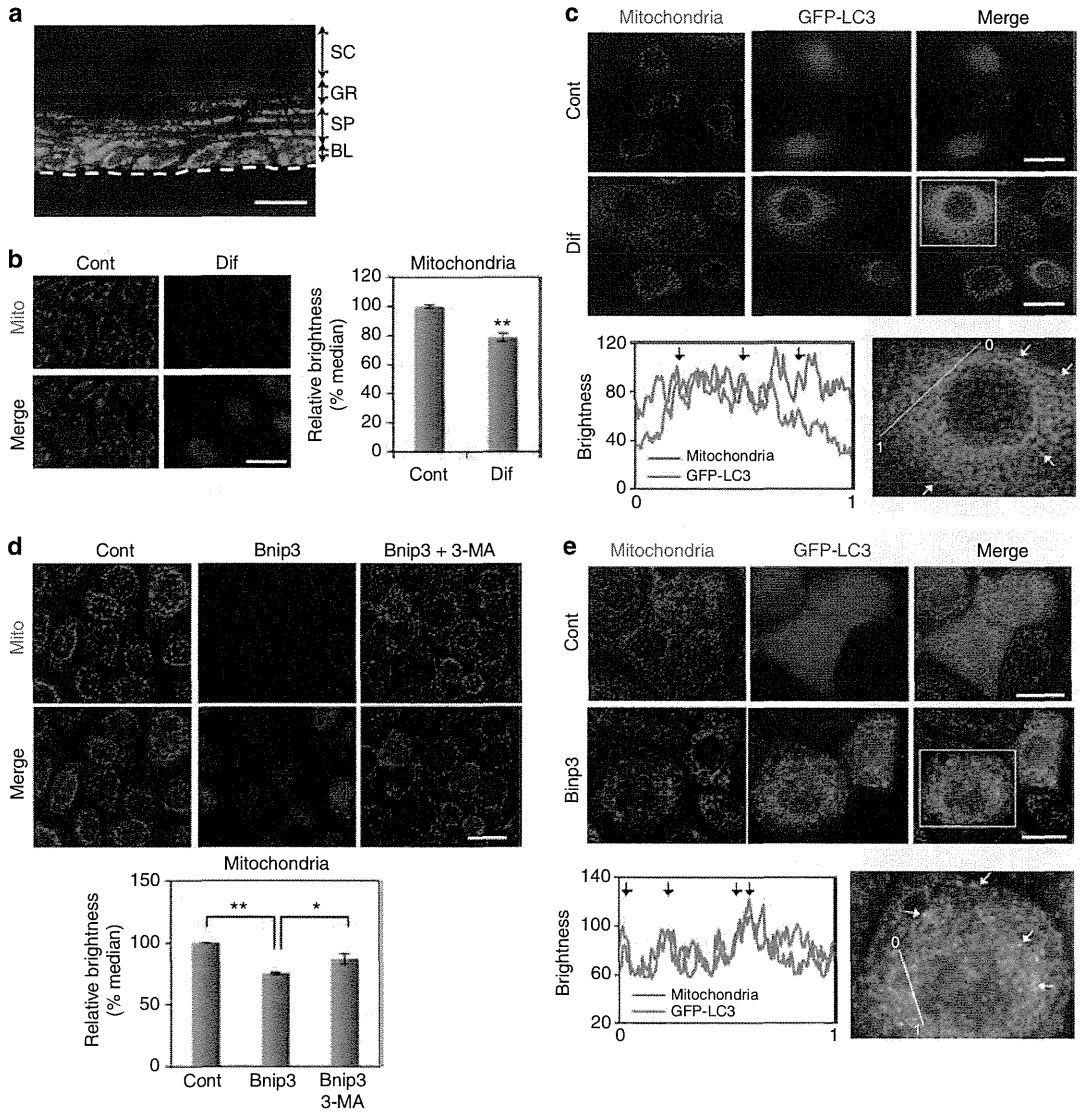

Figure 4. Autophagy stimulates mitochondrial degradation. (**a**) Distribution pattern of mitochondria. The blue signals indicate nuclear staining. The dotted lines indicate the boundary between the epidermis and the membrane. Scale bars = 20 μm. BL, basal layer; GL, granular layer; SC, stratum corneum (cornified layer); SP, spinous layer. (**b**) Nondifferentiated control (Cont) or differentiated human primary epidermal keratinocytes (HPEKs; Dif) were subjected to immunofluorescent staining 2 days after induction of differentiation. Mitochondrial staining is shown in red. The blue signals indicate nuclear staining. Scale bar = 20 μm. The graph indicates the percent of median brightness calculated by BZ Analyzer Software (Keyence) as the mean of three independent experiments ± SD. (**c**) EGFP-LC3-expressing HPEKs were differentiated. Cont or Dif were stained with anti-mitochondria (red) and anti-EGFP (green) 8 hours after induction of differentiation. Graph indicates the linescan analysis of the red and green fluorescent channels. Initial point of linescan is indicated as 0, and terminal point is indicated as 1. The arrows mark the colocalization of the two proteins. (**d**) HPEKs were transduced with enhanced green fluorescent protein (EGFP; Cont) or BNIP3 (BCL2 and adenovirus E1B 19-kDa-interacting protein 3). As an inhibitor of autophagy, 3-methyladenine 3-MA (5 mM) was added. Cells were then fixed and stained with anti-mitochondria 48 hours after transduction. Scale bar = 20 μm. The graph indicates the percent of median brightness calculated by BZ Analyzer Software (Keyence) as the mean of three independent experiments. $^{**}P<0.01$; $^{*}0.01<P<0.05$. (**e**) EGFP-LC3-expressing HPEKs were transduced with mock (Cont) or BNIP3. Cells were then fixed and stained with anti-mitochondria (red) and anti-EGFP (green) 24 hours after transduction. Graph indicates the linescan analysis of the red and green fluorescent channels. Initial point of linescan is indicated as 0, and terminal point is indicated as 1. The arrows mark the colocalization of the two proteins.

DISCUSSION

In this study, we demonstrated that BNIP3, a potent inducer of autophagy, plays a role in the terminal differentiation and maintenance of epidermal keratinocytes. It has been suggested that autophagy plays a role in the skin epidermis, but few attempts have been made to clarify the involvement of autophagy in skin epidermis.

We found that the HES1 transcriptional repressor directly suppressed BNIP3 expression in mouse epidermis and HPEKs (Figure 1). Moreover, our results revealed that BNIP3 was

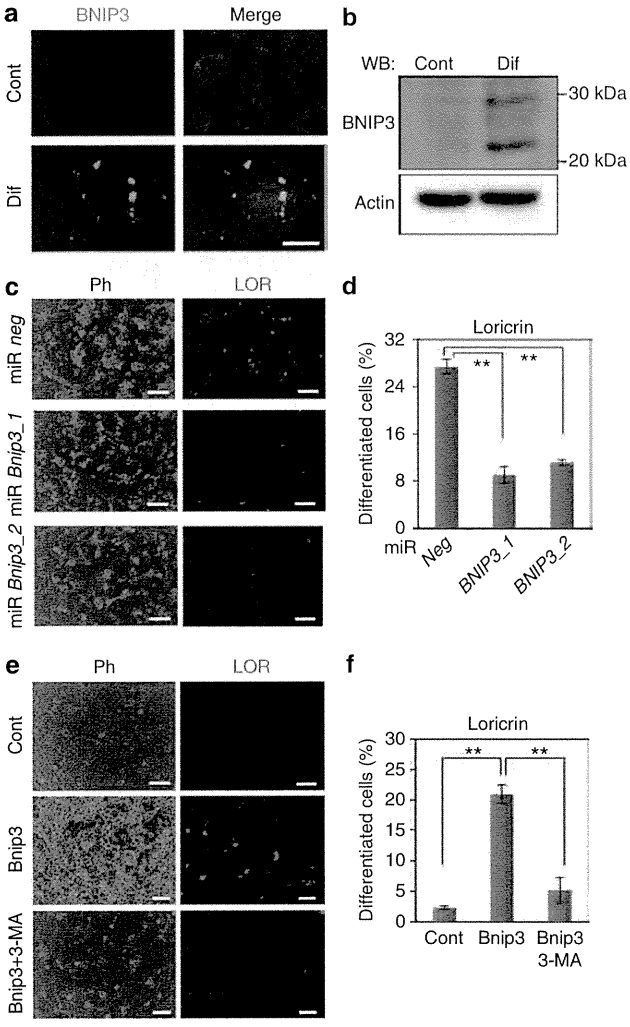

Figure 5. BNIP3 (BCL2 and adenovirus E1B 19-kDa-interacting protein 3) is required for the differentiation of keratinocytes *in vitro*. (**a**, **b**) Human primary epidermal keratinocytes (HPEKs) were differentiated and BNIP3 expression was observed. (**a**) Nondifferentiated control (Cont) or differentiated HPEKs (Dif) were subjected to immunofluorescent staining. BNIP3 staining is shown in green. Mitochondrial staining is shown in red. The blue signals indicate nuclear staining. Scale bar = 20 μm. (**b**) Western blot (WB) analysis. Proteins extracted from Cont or Dif were probed with anti-BNIP3 or anti-actin. (**c**, **d**) HPEKs were infected with adenoviral vectors expressing miR *neg*, miR *BNIP3_1*, or miR *BNIP3_2* followed by induction of differentiation. Cells were then immunostained with a loricrin antibody 9 days after transduction. (**e**, **f**) HPEKs were infected with adenoviral vectors expressing enhanced green fluorescent protein (EGFP; Cont) or BNIP3 and subjected to immunofluorescent staining against loricrin (LOR) 6 days after transduction. As an inhibitor of autophagy, 3-methyladenine 3-MA (5 mM) was added. Phase contrast images (Ph) and LOR staining are shown. Scale bars = 200 μm. (**d**, **f**) Percentages of LOR-positive differentiated cells were calculated by computerized image analysis. The data represent the average of three independent experiments ± SD. $^{**}P<0.01$.

expressed in the granular layers of mouse epidermis, its human skin epidermal equivalent, and its normal human skin epidermis (Figures 1 and 2). These data are consistent with our previous report showing that Hes1 is expressed in the spinous layers, where it represses the regulatory genes for differentiation to maintain the spinous cell fate (Moriyama *et al.*, 2008). Hence, it can be inferred that Bnip3 expression is suppressed in the spinous layers by Hes1, whereas it is upregulated in the granular layers where Hes1 expression is absent. In addition, our finding that BNIP3 is required for keratinocyte differentiation fits our idea that Hes1 represses certain regulatory genes to prevent the premature differentiation of spinous cells. Our *in vitro* data suggest that BNIP3 is involved in keratinocyte differentiation through autophagy (Figures 3–5). The mechanisms underlying the involvement of autophagy in keratinocyte differentiation remain elusive; however, considering that keratinocyte differentiation induced mitochondrial clearance and BNIP3 expression (Figure 4 and 5), BNIP3-induced autophagy may be responsible for the removal of mitochondria that may be required for the terminal differentiation of epidermal keratinocytes. During reticulocyte differentiation, programmed clearance of mitochondria induced by BNIP3L/Nix, a molecule closely related to BNIP3, has been reported to be a critical step (Schweers *et al.*, 2007). Therefore, keratinocytes likely possess the same differentiation mechanism that reticulocytes have, although further investigation will be required for elucidation.

In contrast to the results from differentiation in two-dimensional culture, we did not observe drastic differentiation defects in the BNIP3 knockdown human epidermal equivalent except for the existence of "sunburn-like cells" (Figure 6). This might be because of the incomplete suppression of BNIP3 in the BNIP3 knockdown keratinocytes, and/or might be because of the redundancy between BNIP3 and BNIP3L/Nix, a homolog of BNIP3, as we found in our preliminary study that Bnip3l is also expressed in the epidermis (data not shown). Although the phenotypes of BNIP3-null mice were published in 2007, these researchers found that BNIP3-null mice had no increase in mortality or apparent physical abnormalities (Diwan *et al.*, 2007). Generally, impairment of epidermal differentiation or skin barrier formation results in an obvious defect. Thus, BNIP3-null epidermis seems to exhibit subtle, if any, abnormalities. On the basis of these findings, the involvement of BNIP3 in epidermal differentiation must be investigated in the future. In-depth analysis of the BNIP3-null epidermis phenotype could help elucidate the role of BNIP3 in mouse epidermal differentiation.

Despite the lack of obvious differentiation defects in the human epidermal equivalent, our data showing that BNIP3 knockdown caused the appearance of "sunburn-like cells" is regarded as an example of apoptosis (Young, 1987), revealing a new role of BNIP3 in keratinocyte maintenance. Furthermore, requirement of BNIP3 for protection from UV-induced apoptosis was confirmed in two-dimensional keratinocyte cultures (Figure 6e). The underlying mechanism of this prosurvival function of BNIP3 in keratinocytes remains unclear; however, previous reports have demonstrated that hypoxia-induced autophagy through BNIP3 is critical for the prosurvival process (Bellot *et al.*, 2009). Recently, it has been reported that UVA induces autophagy to remove oxidized phospholipids and protein aggregates in epidermal keratino-

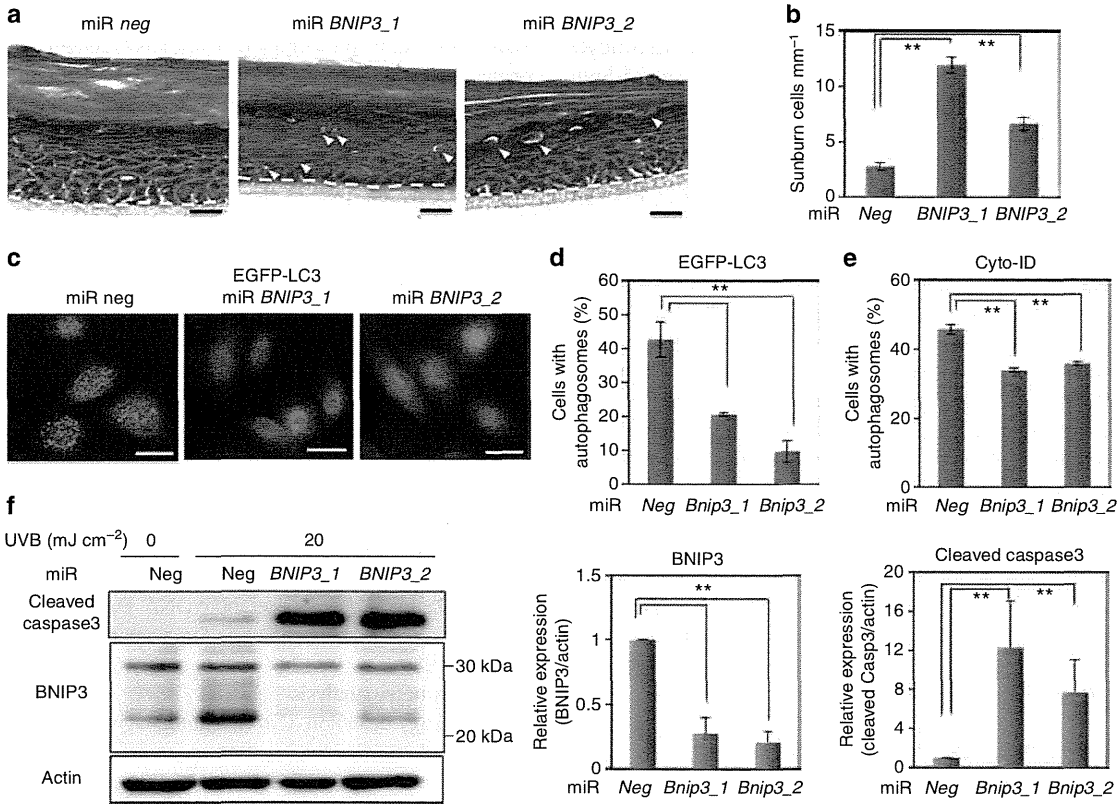

Figure 6. BNIP3 (BCL2 and adenovirus E1B 19-kDa-interacting protein 3) promotes cell survival in the reconstituted epidermis and keratinocytes. (**a**) Morphology of the human skin epidermal equivalents from human primary epidermal keratinocytes (HPEKs) infected with lentivirus expressing miR *neg*, miR *BNIP3_1*, or miR *BNIP3_2*. Arrowheads indicate sunburn-like cells. (**b**) The number of sunburn-like cells per mm was counted and plotted as the means of 10 sections ± SD. (**c–e**) HPEKs were infected with adenovirus expressing miR *neg*, miR *BNIP3_1*, or miR *BNIP3_2*, and irradiated with UVB. (**c**) Cells were stained with anti-EGFP at 8 hours after UVB irradiation. (**d**) The percentage of EGFP-LC3-positive cells with more than five puncta were quantified and are presented as the mean of three independent experiments ± SD. (**e**) Autophagy induction was determined by Cyto-ID staining and quantified by flow cytometry. The data represent the average of three independent experiments ± SD. (**f**) Cells were subjected to western blot analysis at 8 hours after irradiation. The blot shown is representative image of three independent experiments. Graphs indicate relative band intensities as determined by ImageJ software and plotted as the means of three independent experiments. Scale bars = 20 μm. $^{**}P < 0.01$.

cytes (Zhao *et al.*, 2013). Because our data indicate that UVB-induced autophagy is mediated by BNIP3 (Figure 6c and d), it is possible that autophagy induced by BNIP3 also plays a role in the maintenance of keratinocytes. Further analysis is required to confirm these results.

UV-induced apoptotic cells appear within 12 hours and are predominately located in the suprabasal differentiated keratinocyte compartment of human skin (Gilchrest *et al.*, 1981). Moreover, differentiated keratinocytes appear to be most sensitive to the UV light that induces p53-dependent apoptosis (Tron *et al.*, 1998). Tron *et al.* (1998) demonstrated that differentiated keratinocytes in p53-null mice exhibited only a small increase in apoptosis after UVB irradiation compared with the increase observed in normal control animals (Tron *et al.*, 1998). Interestingly, because p53 has been reported to directly suppress BNIP3 expression (Feng *et al.*, 2011), BNIP3 might be abundantly upregulated in suprabasal cells in p53-null animals, resulting in the resistance to UVB-induced apoptosis. Indeed, our preliminary study showed that p53 knockdown enhanced UV-induced BNIP3 expression in HPEKs (data not shown). Therefore, BNIP3 expression in suprabasal cells appears to be important for the protection of differentiated keratinocytes from normal environmental stress such as weak UV exposure *in vivo*.

A recent report on a role for autophagy in epidermal barrier formation and function was identified in *atg7*-deficient mice (Rossiter *et al.*, 2013). The authors showed that autophagy was constitutively active in the suprabasal epidermal layers as we report in this study (Figure 2). However, in contradiction to our results, the authors concluded that autophagy was not essential for the barrier function of the skin. This may be because of the presence of an alternative Atg5/Atg7-independent autophagic pathway (Nishida *et al.*, 2009) in the epidermis. This Atg5/Atg7-independent pathway is also independent of LC3, but forms Rab9-positive double-membrane vesicles. Moreover, protein degradation via this pathway is inhibited by 3-MA and is dependent on Beclin 1. Our data demonstrate that: (1) BNIP3 induced the formation of

EGFP-LC3 puncta (Figure 4) and (2) 3-MA significantly diminished the formation of GFP-LC3 puncta and keratinocyte differentiation induced by BNIP3 (Figure 5). These findings suggest that BNIP3 in the epidermis induced both conventional and Atg5/Atg7-independent autophagy. Intriguingly, GFP cleaved from GFP-LC3 also accumulates in the *Atg7*-deficient epidermis (Rossiter *et al.*, 2013), thereby demonstrating the existence of an alternative autophagic pathway (Juenemann and Reits, 2012) in the epidermis. Further investigation will be required to determine whether Beclin 1 and Rab9 are indispensable for the BNIP3-induced autophagy and subsequent differentiation of keratinocytes.

In summary, our data reveal that expression of BNIP3 in granular cells induces autophagy and is involved in the terminal differentiation and maintenance of skin epidermis. Studies on the involvement of autophagy in skin epidermis have attracted considerable attention recently. In addition, increasing evidence suggests the involvement of BNIP3 in the differentiation of several cell types, including oligodendrocytes (Itoh *et al.*, 2003), osteoclasts (Knowles and Athanasou, 2008), and chondrocytes (Zhao *et al.*, 2012); however, the precise role of BNIP3 in this process remains to be investigated. Our study thus provides new insights into the functions of BNIP3 in differentiation and homeostasis.

MATERIALS AND METHODS

Histology and immunofluorescent analysis

Samples and embryos were fixed in 4% paraformaldehyde, embedded in optimal cutting temperature compound, frozen, and sectioned at 10 μm. Sections were then either subjected to hematoxylin and eosin staining or immunohistochemical analysis as previously described (Moriyama *et al.*, 2006). Details are described in Supplementary Materials Online.

Cell culture

HPEKs were purchased from CELLnTEC (Bern, Switzerland) and maintained in CnT-57 (CELLnTEC) culture medium according to the manufacturer's protocol. For induction of differentiation, the medium was changed to CnT-02 (CELLnTEC) at confluent monolayers of HPEKs, followed by adding calcium ions to 1.8 mM. The generation of human skin equivalents was performed using CnT-02-3DP culture medium (CELLnTEC) according to the manufacturer's protocol.

Design of artificial microRNAs and plasmid construction

Oligonucleotides targeting a human BNIP3 sequence compatible for use in cloning into BLOCK-iT Pol II miR RNAi expression vectors (Invitrogen, Carlsbad, CA) were obtained using the online tool BLOCK-iT RNAi Designer. The oligonucleotide sequences used in this study are shown in Supplementary Table S1 online. Cloning procedures were performed following the manufacturer's instructions.

Adenovirus and lentivirus infection

Adenoviruses expressing EGFP, Hes1, BNIP3, and miR *BNIP3* were constructed using the ViraPower adenoviral expression system (Invitrogen) according to the manufacturer's protocol. Lentivirus expressing EGFP-LC3 (from Addgene plasmid 21073, Cambridge, MA) and miR *BNIP3* plasmid was constructed and used to infect keratinocytes as previously described (Moriyama *et al.*, 2012; Moriyama *et al.*, 2013).

RNA extraction, complementary DNA generation, and Q-PCR

Total RNA extraction, complementary DNA generation, and Q-PCR analyses were carried out as previously described (Moriyama *et al.*, 2012). Details of the primers used in these experiments are shown in Supplementary Table S2 online.

Western blot analysis

Western blot analysis was performed as previously described (Moriyama *et al.*, 2012; Moriyama *et al.*, 2013). Details are described in Supplementary Materials Online.

ChIP assay

The ChIP assay was performed using the SimpleChIP Enzymatic Chromatin IP Kit (Magnetic Beads) (Cell Signaling Technology, Danvers, MA) according to the manufacturer's instructions. Hemagglutinin-tagged Hes1 was immunoprecipitated with rabbit polyclonal antibody against hemagglutinin tag (ab9110, Abcam, Cambridge, MA). Immunoprecipitated DNA was analyzed by Q-PCR. Relative quantification using a standard curve method was performed, and the occupancy level for a specific fragment was defined as the ratio of immunoprecipitated DNA over input DNA. Details of the primers used in these experiments are shown in Supplementary Table S2 online.

Flow cytometry analysis

For autophagy detection, Cyto-ID Autophagy detection kit (Enzo Life Sciences, Plymouth Meeting, PA) was used according to the manufacturer's instructions. Details are described in Supplementary Materials Online.

CONFLICT OF INTEREST

The authors state no conflict of interest.

ACKNOWLEDGMENTS

We thank Shogo Nomura, Ayumi Kitagawa, and Riho Ishihama for technical support; Dr Takashi Ueno for helpful discussions; Dr Hiroyuki Miyoshi for the CSII-EF-RfA, pCMV-VSVG-RSV-Rev, and pCAG-HIVg/p plasmids; Dr Tamotsu Yoshimori for pEGFP-LC3 plasmid; and Dr Ryoichiro Kageyama for *Hes1* KO mice. This work was supported by MEXT KAKENHI grant 23791304 to MM. This work was also supported in part by grants from the Ministry of Health, Labor, and Welfare of Japan and a grant from the Program for Promotion of Fundamental Studies in Health Sciences of the National Institute of Biomedical Innovation (NIBIO).

SUPPLEMENTARY MATERIAL

Supplementary material is linked to the online version of the paper at http://www.nature.com/jid

REFERENCES

Aymard E, Barruche V, Naves T *et al.* (2011) Autophagy in human keratinocytes: an early step of the differentiation? *Exp Dermatol* 20:263–8

Bellot G, Garcia-Medina R, Gounon P *et al.* (2009) Hypoxia-induced autophagy is mediated through hypoxia-inducible factor induction of BNIP3 and BNIP3L via their BH3 domains. *Mol Cell Biol* 29:2570–81

Blanpain C, Lowry WE, Pasolli HA *et al.* (2006) Canonical notch signaling functions as a commitment switch in the epidermal lineage. *Genes Dev* 20:3022–35

Chan LL, Shen D, Wilkinson AR *et al.* (2012) A novel image-based cytometry method for autophagy detection in living cells. *Autophagy* 8:1371–82

Chatterjea SM, Resing KA, Old W *et al.* (2011) Optimization of filaggrin expression and processing in cultured rat keratinocytes. *J Dermatol Sci* 61:51–9

Diwan A, Krenz M, Syed FM *et al.* (2007) Inhibition of ischemic cardiomyocyte apoptosis through targeted ablation of Bnip3 restrains postinfarction remodeling in mice. *J Clin Invest* 117:2825–33

Feng X, Liu X, Zhang W *et al.* (2011) p53 directly suppresses BNIP3 expression to protect against hypoxia-induced cell death. *EMBO J* 30: 3397–415

Gilchrest BA, Soter NA, Stoff JS *et al.* (1981) The human sunburn reaction: histologic and biochemical studies. *J Am Acad Dermatol* 5:411–22

Hamacher-Brady A, Brady NR, Logue SE *et al.* (2007) Response to myocardial ischemia/reperfusion injury involves Bnip3 and autophagy. *Cell Death Differ* 14:146–57

Haruna K, Suga Y, Muramatsu S *et al.* (2008) Differentiation-specific expression and localization of an autophagosomal marker protein (LC3) in human epidermal keratinocytes. *J Dermatol Sci* 52:213–5

Ishibashi M, Moriyoshi K, Sasai Y *et al.* (1994) Persistent expression of helix-loop-helix factor HES-1 prevents mammalian neural differentiation in the central nervous system. *EMBO J* 13:1799–805

Itoh T, Itoh A, Pleasure D (2003) Bcl-2-related protein family gene expression during oligodendroglial differentiation. *J Neurochem* 85:1500–12

Juenemann K, Reits EA (2012) Alternative macroautophagic pathways. *Int J Cell Biol* 2012:189794

Kabeya Y, Mizushima N, Ueno T *et al.* (2000) LC3, a mammalian homologue of yeast Apg8p, is localized in autophagosome membranes after processing. *EMBO J* 19:5720–8

Knowles HJ, Athanasou NA (2008) Hypoxia-inducible factor is expressed in giant cell tumour of bone and mediates paracrine effects of hypoxia on monocyte-osteoclast differentiation via induction of VEGF. *J Pathol* 215:56–66

Lippens S, Denecker G, Ovaere P *et al.* (2005) Death penalty for keratinocytes: apoptosis versus cornification. *Cell Death Differ* 12(Suppl 2):1497–508

Mellor HR, Rouschop KM, Wigfield SM *et al.* (2010) Synchronised phosphorylation of BNIP3, Bcl-2 and Bcl-xL in response to microtubule-active drugs is JNK-independent and requires a mitotic kinase. *Biochem Pharmacol* 79:1562–72

Mizushima N, Levine B (2010) Autophagy in mammalian development and differentiation. *Nat Cell Biol* 12:823–30

Mizushima N, Yamamoto A, Matsui M *et al.* (2004) In vivo analysis of autophagy in response to nutrient starvation using transgenic mice expressing a fluorescent autophagosome marker. *Mol Biol Cell* 15:1101–11

Mizushima N, Yoshimori T, Levine B (2010) Methods in mammalian autophagy research. *Cell* 140:313–26

Moriyama H, Moriyama M, Sawaragi K *et al.* (2013) Tightly regulated and homogeneous transgene expression in human adipose-derived mesenchymal stem cells by lentivirus with tet-off system. *PLoS One* 8:e66274

Moriyama M, Durham AD, Moriyama H *et al.* (2008) Multiple roles of Notch signaling in the regulation of epidermal development. *Dev Cell* 14:594–604

Moriyama M, Moriyama H, Ueda A *et al.* (2012) Human adipose tissue-derived multilineage progenitor cells exposed to oxidative stress induce neurite outgrowth in PC12 cells through p38 MAPK signaling. *BMC Cell Biol* 13:21

Moriyama M, Osawa M, Mak SS *et al.* (2006) Notch signaling via Hes1 transcription factor maintains survival of melanoblasts and melanocyte stem cells. *J Cell Biol* 173:333–9

Nishida Y, Arakawa S, Fujitani K *et al.* (2009) Discovery of Atg5/Atg7-independent alternative macroautophagy. *Nature* 461:654–8

Ohtsuka T, Ishibashi M, Gradwohl G *et al.* (1999) Hes1 and Hes5 as notch effectors in mammalian neuronal differentiation. *EMBO J* 18:2196–207

Quinsay MN, Thomas RL, Lee Y *et al.* (2010) Bnip3-mediated mitochondrial autophagy is independent of the mitochondrial permeability transition pore. *Autophagy* 6:855–62

Rossiter H, Konig U, Barresi C *et al.* (2013) Epidermal keratinocytes form a functional skin barrier in the absence of Atg7 dependent autophagy. *J Dermatol Science* 71:67–75

Sassone J, Colciago C, Marchi P *et al.* (2010) Mutant Huntingtin induces activation of the Bcl-2/adenovirus E1B 19-kDa interacting protein (BNip3). *Cell Death Dis* 1:e7

Schweers RL, Zhang J, Randall MS *et al.* (2007) NIX is required for programmed mitochondrial clearance during reticulocyte maturation. *Proc Natl Acad Sci USA* 104:19500–5

Sowter HM, Ratcliffe PJ, Watson P *et al.* (2001) HIF-1-dependent regulation of hypoxic induction of the cell death factors BNIP3 and NIX in human tumors. *Cancer Res* 61:6669–73

Srinivas V, Bohensky J, Shapiro IM (2009) Autophagy: a new phase in the maturation of growth plate chondrocytes is regulated by HIF, mTOR and AMP kinase. *Cells Tissues Organs* 189:88–92

Tron VA, Trotter MJ, Tang L *et al.* (1998) p53-regulated apoptosis is differentiation dependent in ultraviolet B-irradiated mouse keratinocytes. *Am J Pathol* 153:579–85

Vengellur A, LaPres JJ (2004) The role of hypoxia inducible factor 1alpha in cobalt chloride induced cell death in mouse embryonic fibroblasts. *Toxicol Sci* 82:638–46

Walls KC, Ghosh AP, Ballestas ME *et al.* (2009) bcl-2/Adenovirus E1B 19-kd interacting protein 3 (BNIP3) regulates hypoxia-induced neural precursor cell death. *J Neuropathol Exp Neurol* 68:1326–38

Young AR (1987) The sunburn cell. *Photodermatology* 4:127–34

Zhang J, Ney PA (2009) Role of BNIP3 and NIX in cell death, autophagy, and mitophagy. *Cell Death Differ* 16:939–46

Zhao Y, Chen G, Zhang W *et al.* (2012) Autophagy regulates hypoxia-induced osteoclastogenesis through the HIF-1alpha/BNIP3 signaling pathway. *J Cell Physiol* 227:639–48

Zhao Y, Zhang CF, Rossiter H *et al.* (2013) Autophagy is induced by UVA and promotes removal of oxidized phospholipids and protein aggregates in epidermal keratinocytes. *J Invest Dermatol* 133:1629–37

STEM CELLS AND DEVELOPMENT
Volume 23, Number 18, 2014

DOI: 10.1089/scd.2013.0642

Role of Notch Signaling in the Maintenance of Human Mesenchymal Stem Cells Under Hypoxic Conditions

Hiroyuki Moriyama,[1,*] Mariko Moriyama,[1,*] Haruki Isshi,[1] Shin Ishihara,[1] Hanayuki Okura,[2] Akihiro Ichinose,[3] Toshiyuki Ozawa,[4] Akifumi Matsuyama,[2] and Takao Hayakawa[1]

Human adipose tissue-derived multilineage progenitor cells (hADMPCs) are attractive for cell therapy and tissue engineering because of their multipotency and ease of isolation without serial ethical issues. However, their limited in vitro lifespan in culture systems hinders their therapeutic application. Some somatic stem cells, including hADMPCs, are known to be localized in hypoxic regions; thus, hypoxia may be beneficial for ex vivo culture of these stem cells. These cells exhibit a high level of glycolytic metabolism in the presence of high oxygen levels and further increase their glycolysis rate under hypoxia. However, the physiological role of glycolytic activation and its regulatory mechanisms are still incompletely understood. Here, we show that Notch signaling is required for glycolysis regulation under hypoxic conditions. Our results demonstrate that 5% O_2 dramatically increased the glycolysis rate, improved the proliferation efficiency, prevented senescence, and maintained the multipotency of hADMPCs. Intriguingly, these effects were not mediated by hypoxia-inducible factor (HIF), but rather by the Notch signaling pathway. Five percent O_2 significantly increased the level of activated Notch1 and expression of its downstream gene, *HES1*. Furthermore, 5% O_2 markedly increased glucose consumption and lactate production of hADMPCs, which decreased back to normoxic levels on treatment with a γ-secretase inhibitor. We also found that HES1 was involved in induction of GLUT3, TPI, and PGK1 in addition to reduction of TIGAR and SCO2 expression. These results clearly suggest that Notch signaling regulates glycolysis under hypoxic conditions and, thus, likely affects the cell lifespan via glycolysis.

Introduction

HUMAN ADIPOSE TISSUE-DERIVED mesenchymal stem cells (MSCs), also referred to as human adipose tissue-derived multilineage progenitor cells (hADMPCs), are multipotent stem cells that can differentiate into various types of cells, including hepatocytes [1], cardiomyoblasts [2], pancreatic cells [3], and neuronal cells [4–6]. They can be easily and safely obtained from lipoaspirate without posing serious ethical issues and can also be expanded ex vivo under appropriate culture conditions. Moreover, MSCs, including hADMPCs, have the ability to migrate to injured areas and secrete a wide variety of cytokines and growth factors that are necessary for tissue regeneration [7–11]. In addition, due to their hypoimmunogenicity and immunomodulatory effects, hADMPCs are good candidates as gene delivery vehicles for therapeutic purposes [12]. Thus, hADMPCs are attractive seeding cells for cell therapy and tissue engineering. However, similar to other somatic stem cells or primary cells, hADMPCs have limited growth potential and ultimately stop proliferation as a result of cellular senescence [13], which hinders their therapeutic application.

Conversely, embryonic stem cells (ESCs) and induced pluripotent stem cells (iPSCs) are immortal under standard culture conditions. Recently, several groups have reported that these cells greatly rely on glycolysis for energy production even under high-oxygen conditions [14–16]. This phenomenon is known as the Warburg effect and was originally described for cancer cells by Otto Warburg in the 1920s [17]. Although mitochondrial respiration is more efficient than glycolysis in generating ATP (net yield of 30 ATPs vs. 2 ATPs), glycolysis is able to produce ATP considerably faster than mitochondrial respiration as long as glucose supplies are adequate. Thus, a metabolic shift from mitochondrial respiration to glycolysis would provide a growth advantage for actively proliferating cells. Moreover, Kondoh et al. demonstrated that enhanced glycolysis is also involved in cellular immortalization through reduction of

[1]Pharmaceutical Research and Technology Institute, Kinki University, Higashi-Osaka, Osaka, Japan.
[2]Platform of Therapeutics for Rare Disease and Health Policy, National Institute of Biomedical Innovation, Kobe, Japan.
[3]Department of Plastic Surgery, Kobe University Hospital, Kobe, Japan.
[4]Department of Dermatology, Graduate School of Medicine, Osaka City University, Osaka, Japan.
*These two authors contributed equally to this work.

intrinsic reactive oxygen species (ROS) production [14,18,19]. Since accumulation of intrinsic ROS levels could be a major reason for replicative senescence [20], enhancing glycolysis in cultured cells might improve the quality of the cells by suppressing premature senescence. One candidate method for induction of glycolysis is application of low-oxygen conditions to activate the transcription factor, hypoxia-inducible factor (HIF). HIF-1 is known to increase the expression of most glycolytic enzymes and the glucose transporters GLUT1 and GLUT3 [20]. Thus, several studies have reported that hypoxia is beneficial for the maintenance of hESCs in a pluripotent state [21,22]. Moreover, low oxygen tension has been reported to enhance the generation of iPSCs both from mouse and human primary fibroblasts [23].

Recently, hypoxic culture conditions have also been reported to confer a growth advantage, prevent premature senescence, and maintain undifferentiated states in somatic stem cells; for example, hematopoietic stem cells (HSCs) [24], neural stem cells [25], and bone marrow-derived MSCs [26]. These stem cells reside in their local microenvironments called the "stem cell niche," where the oxygen tension is relatively low (in the range of 1%–9%). Thus, hypoxic culture may be beneficial to these stem cells with regard to in vitro proliferation, cell survival, and differentiation. Takubo et al. reported that HSCs activated Pdk through HIF1α in hypoxic culture conditions, resulting in maintenance of glycolytic flow and suppression of the influx of glycolytic metabolites into mitochondria, and this glycolytic metabolic state was shown to be indispensable for the maintenance of HSCs [27]. Several studies have reported that MSCs exhibit a high level of glycolytic metabolism in the presence of high oxygen levels and further increase their rate of glycolysis on culture under hypoxia [28,29]. However, a relationship between beneficial effects of hypoxic conditions and metabolic status in addition to involvement of HIFs in the metabolic changes has not been investigated in these reports.

In this study, we aimed at investigating the effect of 5% oxygen on hADMPCs. Our results demonstrate that culture under 5% oxygen increased the glycolysis rate, improved the proliferation efficiency, prevented the cellular senescence, and maintained the undifferentiated status of hADMPCs. Intriguingly, these effects were not mediated by HIF, but rather by Notch signaling, an important signaling pathway required for the development of many cell types and maintenance of stem cells [30,31]. Five percent oxygen activated Notch signaling, resulting in the upregulation of *SLC2A3*, *TPI*, and *PGK1* in addition to the downregulation of *TIGAR* and *SCO2*, which may contribute to the increase in the glycolysis rate. These observations, thus, provide new regulatory mechanisms for stemness maintenance obtained under 5% oxygen conditions.

Materials and Methods

Adipose tissue samples

Subcutaneous adipose tissue samples (10–50 g each) were resected during plastic surgery from five female and two male patients (age 20–60 years) as discarded tissue. The study protocol was approved by the Review Board for Human Research of Kobe University Graduate School of Medicine Foundation for Biomedical Research and Innovation, Osaka City University Graduate School of Medicine, and Kinki University Pharmaceutical Research and Technology Institute (reference number: 12-043). Each subject provided signed informed consent.

Cell culture

hADMPCs were isolated as previously reported [11,32–34] and maintained in a medium containing 60% DMEM low glucose, 40% MCDB-201 medium (Sigma Aldrich), 1× insulin-transferrin-selenium (Life Technologies), 1 nM dexamethasone (Sigma Aldrich), 100 mM ascorbic acid 2-phosphate (Wako), 10 ng/mL epidermal growth factor (PeproTech), and 5% fetal bovine serum. The cells were plated to a density of 5×10^3 cells/cm^2 on fibronectin-coated dishes, and the medium was replaced every 2 days. For hypoxic culture, cells were cultured in a gas mixture composed of 90% N_2, 5% CO_2, and 5% O_2. For maintenance of the hypoxic gas mixture, a ProOx C21 carbon dioxide and oxygen controller and a C-Chamber (Biospherix) were used.

Senescence-associated β-galactosidase staining

Cells were fixed with 2% paraformaldehyde/0.2% glutaradehyde for 5 min at room temperature and then washed twice with phosphate-buffered saline (PBS). The cells were then incubated overnight at 37°C with fresh senescence-associated β-galactosidase (SA-β-Gal) chromogenic substrate solution (1 mg/mL Bluo-gal (Life Technologies), 40 mM citric acid (pH 6.0), 5 mM potassium ferrocyanide, 5 mM potassium ferricyanide, 150 mM NaCl, and 2 mM $MgCl_2$).

Measurement of ROS production

Cells were harvested and incubated with 10 μM 5-(and-6)-chloromethyl-2′,7′-dichlorodihydrofluorescein diacetate, acetyl ester (CM-H_2DCFDA). The amount of intracellular ROS production was proportional to the green fluorescence, as analyzed using a Guava EasyCyte 8HT flow cytometer (Millipore) using an argon laser at 488 nm and a 525/30 nm band pass filter, and dead cells were excluded using the Live/Dead Fixable Far Red Dead Cell Stain Kit (Life Technologies).

EdU proliferation assay

For assessment of cell proliferation, hADMPCs were seeded on a fibronectin-coated six-well plate at a density of 5×10^3 cells/cm^2 and cultured for 3 days. Cell proliferation was detected by incorporating of 5-ethynyl-2′-deoxyuridine (EdU) and using the Click-iT EdU Alexa Fluor 488 Flow Cytometry Assay Kit (Life Technologies). Briefly, according to the manufacturer's protocol, cells were incubated with 10 μM EdU for 2 h before fixation, permeabilized, and stained with EdU. EdU-positive cells were then analyzed using the 488 nm laser of a Guava EasyCyte 8HT flow cytometer (Millipore).

Flow cytometry analysis

Flow cytometry analysis was performed as previously described [34]. Briefly, hADMPCs were harvested and resuspended in staining buffer (PBS containing 1% BSA, 2 mM EDTA, and 0.01% sodium azide) at a density of